IOP Publishing Superconductor Science and Technology
Supercond. Sci. Technol. 32 (2019) 033001 (33pp) https://doi.org/10.1088/1361-6668/aafc82

Topical Review

Status of CORC® cables and wires for use in high-field magnets and power systems a decade after their introduction

D C van der Laan[1,2,3], J D Weiss[1,2] and D M McRae[1,2]

[1] Advanced Conductor Technologies LLC, Boulder CO 80301, United States of America
[2] Department of Physics, University of Colorado, Boulder, CO 80309, United States of America

E-mail: danko@advancedconductor.com

Received 21 October 2017, revised 7 December 2018
Accepted for publication 8 January 2019
Published 12 February 2019

Abstract

High-field, low-inductance superconducting magnets in particle accelerators and fusion machines require high operating currents, often in combination with high current densities and for some applications conductor bending radii of less than 50 mm. These requirements form a major challenge for magnet conductors consisting of high-temperature superconductors, which are required for reaching magnetic fields exceeding 20 T, or allowing for operating temperatures above 20 K. The high tolerance of RE-$Ba_2Cu_3O_{7-\delta}$ coated conductors to axial tensile and compressive strain has led to the concept of CORC® cables in an attempt to develop a round and mechanically as well as electrically isotropic, high-performance conductor that would meet these challenging requirements. This review article will outline how CORC® cables evolved from a concept into a practical and robust conductor for high-field magnets and compact superconducting power cables. This review article provides an extensive overview of how CORC® cable technology has overcome most of the challenges associated with its use in large magnets for fusion, particle accelerators and in helium gas cooled power and fault current limiting cables, while further development is ongoing that will push the CORC® cable technology to even higher performance levels.

Keywords: REBCO cables, CORC cable, CORC wire

(Some figures may appear in colour only in the online journal)

1. Introduction

The initial development of RE-$Ba_2Cu_3O_{7-\delta}$ (REBCO) coated conductors focused on achieving cost effective, long-length REBCO tapes for application in the electric power grid. A substantial development program supported by the US Department of Energy resulted in several demonstrations of REBCO-based power cables, which clearly underlined the potential of the technology for use in large, liquid nitrogen cooled cables [1–3]. Overall conductor and cryogenic system costs and unproven long-term system reliability prevented electric power utilities in the US to adopt high-temperature superconductors (HTS). Since those early days, markets for which HTS is a true enabling technology, such as for high-field magnets, have become the main driving forces behind REBCO development.

Several HTS materials besides REBCO coated conductors are being developed for use in high-field magnets; including $Bi_2Sr_2Ca_2Cu_3O_x$ (Bi-2223) tapes [4, 5] and $Bi_2Sr_2CaCu_2O_x$ (Bi-2212) wires [6, 7]. The high mechanical strength of REBCO coated conductors that contain stainless steel or Hastelloy substrates, with respect to tensile yield stress and overall axial strain range at which the conductors can be operated, in combination with their very high current densities, have resulted in the successful demonstrations of high-field magnets [8–10]. These magnets were wound from single tapes, carrying no more than a few hundred Amperes of

[3] Author to whom any correspondence should be addressed.

 © 2019 IOP Publishing Ltd Printed in the UK

current, resulting in a relatively high magnet inductance that make burnout at local defects a concrete risk. Other disadvantages of using single tapes to wind magnets include their high aspect ratio, making them hard to bend in plane, and the anisotropy of the critical current (I_c) with respect to magnetic field angle. Round, fully isotropic conductors would be highly beneficial for most magnet applications. Large, low-inductive magnets in which the magnetic field is ramped at relatively high rates require much higher operating currents of several kilo-Amperes that cannot be achieved by single tape conductors.

The concept of the Conductor on Round Core (CORC®) cable originated from the realization that the combination of a strong metal substrate and an almost single-crystalline HTS film in REBCO coated conductors results in a conductor capable of withstanding high axial tensile, and more importantly, compressive strains [11–14]. The high elastic nature of the REBCO film under axial compression allowed for winding large numbers of tapes onto relatively small formers, resulting in thin cables with operating currents that far exceed 1000 A [15]. Being a thin cable in which tapes are wound at short twist pitches, while allowing them to slide during cable bending, has resulted in CORC® cables becoming one of the most flexible HTS conductors to date. CORC® cables are the first round, fully isotropic with regard to bending and of applied magnetic field angle, REBCO-based conductors that allow for high operating currents and engineering current densities (J_e). They have become one of the most practical HTS conductors for use in large high-field magnets and compact power cable systems [16, 17].

This review article provides an in-depth overview of the basic science that allowed for the introduction of CORC® cables and a number of the key developments required to overcome some of the main technical challenges associated with their use in practical applications. These developments include cable terminations that enable homogeneous current injection into the CORC® conductor, increasing the current density at high magnetic fields, and improvement of the mechanical strength of CORC® conductors to ensure reliable operation at high stresses in high-field magnets. Initial application of CORC® conductors will be discussed; including their use in helium gas cooled power and fault current limiting (FCL) cables and in canted cosine-theta accelerator magnets.

2. CORC® cables and wires

2.1. Introduction of the CORC® concept

The deposition of the superconducting film onto thin metal substrates in REBCO coated conductors resulted in a highly elastic conductor in which the REBCO layer can withstand significant axial strain levels (ε) before its critical current degrades irreversibly. In axial tension, the critical current of typical REBCO coated conductors degrades irreversibly only once the metal substrate yields, which is at an applied strain between 0.4% and 0.7% depending on the substrate composition [11, 12, 18]. The critical current changes reversibly

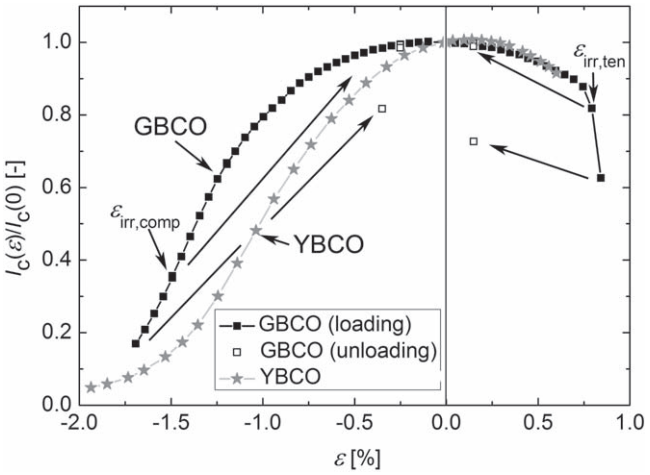

Figure 1. Dependence of the normalized I_c of $GdBa_2Cu_3O_{7-\delta}$ (GBCO) and $YBa_2Cu_3O_{7-\delta}$ (YBCO) coated conductors on axial strain at 76 K. The results include data taken on the GBCO sample after the strain was unloaded. Reproduced from [15]. © IOP Publishing Ltd. All rights reserved.

even before the irreversible strain limit (ε_{irr}) is reached [19], originating from the change in critical temperature (T_c) with lattice strain [20]. A key discovery that allowed for the introduction of CORC® cables was that the irreversible strain limit of REBCO coated conductors under axial compression is about twice as high as under axial tension [13, 21]. Figure 1 shows an example of the strain dependence of I_c of two REBCO coated conductors, including the irreversible strain limit under axial tension ($\varepsilon_{irr,tension}$) and compression ($\varepsilon_{irr,comp}$), defined by the applied strain at which I_c no longer fully recovers after the strain is released.

HTS cables were initially designed with relatively large formers or cores of at least 40 mm in diameter [1–3] onto which Bi-2223 tapes and later REBCO coated conductors were wound. Large formers were required to prevent the winding strain to exceed the irreversible strain limit of Bi-2223 tapes, which is in the order of 0.2%–0.4% under axial tension and only about −0.1% under compression [22, 23]. The size of the former remained unchanged after these cables were wound from REBCO coated conductors instead of Bi-2223 tapes, even though these highly elastic conductors could withstand much higher winding strains.

The high level of elasticity of the REBCO layer under axial compression allowed the use of much thinner formers in HTS cables that ultimately led to the CORC® cable concept [13]. Instead of winding the REBCO tapes with the superconducting film facing outward, exposing the film to axial tensile strain, the REBCO tapes were wound with the superconducting film facing the former. This orientation results in the REBCO film being subjected to axial compressive strain, allowing a strain of at least −1.25% before mechanical degradation occurs. The first proof-of-principle of the CORC® concept was demonstrated by winding a single REBCO coated conductor containing a 50 μm thick substrate and a 20 μm thick layer of surround plated copper at different winding angles onto a 3.2 mm diameter brass rod [13] (figure 2).

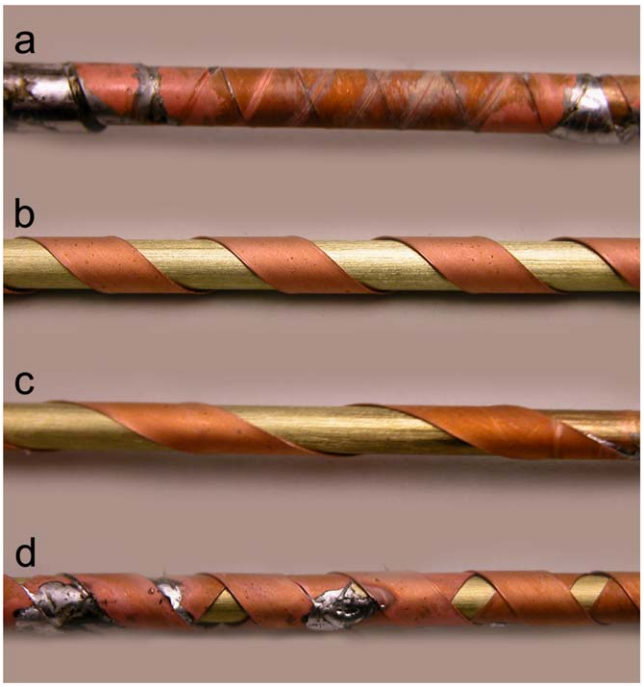

Figure 2. Proof-of-principle CORC® cable prototypes with REBCO tapes wound on a 3.2 mm brass former. A single 4 mm wide REBCO tape wound at a winding angle of (a) 24°, (b) 45° and (c) 63°. (d) Two 4 mm wide tapes wound into two layers at an angle of about 42°. Picture taken on 29 December 2008 and reproduced from [13]. © IOP Publishing Ltd. All rights reserved.

It was unknown at the time of the first CORC® cable tests in 2008–2009 that the 3.2 mm diameter former thickness likely resulted in I_c degradation of the tapes because the maximum axial compressive strain in the REBCO layer, oriented normal to the former, exceeded −1.25%. The maximum REBCO strain, which is a result of bending the REBCO tape over the former, is calculated using the following equation:

$$\varepsilon = \frac{-x}{d + x + 2t}, \tag{1}$$

which depends on the former diameter d, the substrate thickness x and the thickness of the copper plating t [14]. The maximum strain in the RBECO layer of the CORC® cables shown in figure 2 was −1.52%.

Another important factor that likely influenced the tape performance in the CORC® cables of figure 2 was their winding angle. Also unknown at the time was that the magnitude of the reversible strain effect in REBCO coated conductors depends on the in-plane orientation at which the strain is applied, and thus the winding angle of the tapes in CORC® cables. The existence of an anisotropic in-plane reversible strain effect in REBCO coated conductors was only discovered in 2011 [20]. The power-law strain dependence of the critical current in REBCO coated conductors produced with the IBAD-MOCVD method, for instance, is often described with the following equation [21, 24, 25]:

$$I_c(\varepsilon, \alpha) = I_c(\varepsilon_m)(1 - a(\alpha)\,|\varepsilon - \varepsilon_m(\alpha)|^{2.18}), \tag{2}$$

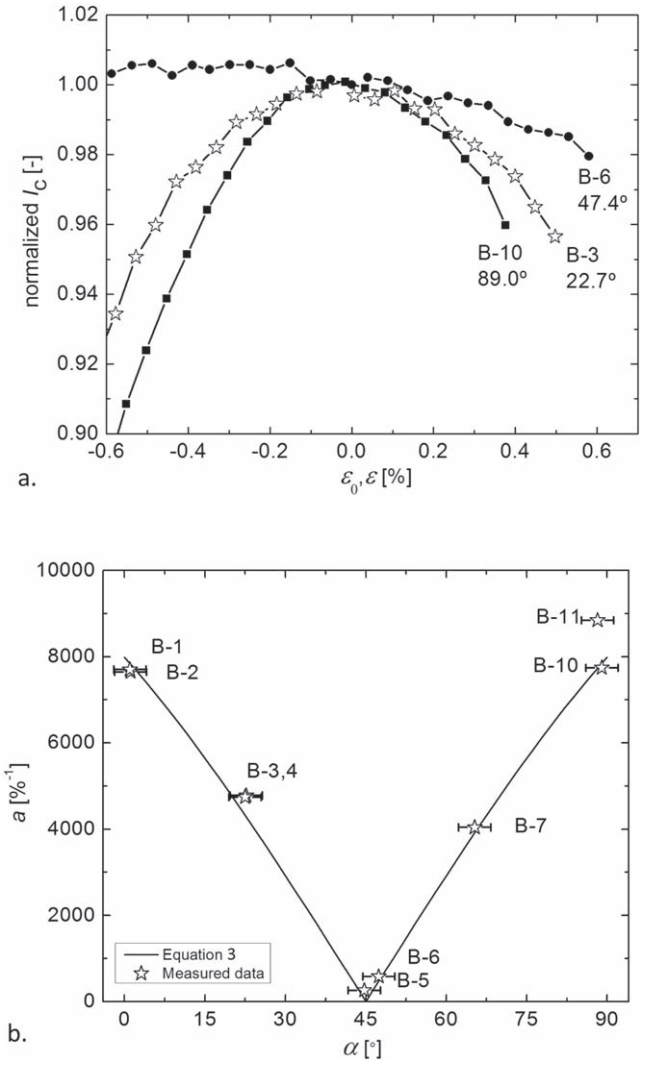

Figure 3. (a) Dependence of the normalized I_c at 76 K of bridges patterned at different angles with respect to the tape axis of REBCO coated conductors. (b) Dependence of the strain sensitivity parameter a on angle as described by equation (3) of the bridges patterned at different angles. The sample numbers indicate the different bridges that were patterned at different angles into the REBCO layers of the samples. Reproduced from [20]. © IOP Publishing Ltd. All rights reserved.

where parameter a represents the strain sensitivity of I_c and $I_c(\varepsilon_m)$ is the maximum critical current occurring at an applied strain ε_m. It was demonstrated that the magnitude of the reversible strain effect on I_c depends on the in-plane angle at which the strain is applied (figure 3) by applying strain to bridges that were patterned into REBCO coated conductors at different angles α with respect to the [100] and [010] directions of the superconducting film [20]. The strain parameter a in equation (2) thus depends on the angle α (figure 3(b)):

$$a(\alpha) = a(0°)|\cos(\alpha) - \sin(\alpha)|. \quad (0 \leqslant \alpha \leqslant 90). \tag{3}$$

Parameter $a(0°)$ $(=a(90°))$ is the maximum strain sensitivity that occurs when the applied strain is oriented parallel to the [100] and [010] directions of the superconducting film, which in most REBCO coated conductors coincides with the

Figure 4. A 3 mm wide superconducting tape containing a 30 μm thick substrate wound onto a 2.8 mm diameter former. A 3 mm wide copper tape is wound in parallel to the superconducting tape to ensure a constant winding angle close to 45°. Reproduced from [26]. © IOP Publishing Ltd. All rights reserved.

tape axis, and is equal to about 7985 for the sample highlighted in figure 3. The REBCO film in tapes produced with the IBAD-MOCVD route is aligned with their *a*- and *b*-axis along the tape direction, and due to twinning, normal to the tape axis.

The benefits of the anisotropic reversible strain effect for CORC® cables are substantial. The reversible reduction in I_c at −1% axial strain applied along the tape axis is between about 20%–50% depending on the REBCO composition (figure 1). The tape performance when wound into a CORC® cable would thus be reduced significantly. The anisotropic strain effect in coated conductors causes the reversible stain effect in most conductors to disappear almost completely, and I_c to become independent of strain, when strain is applied at an angle of 45° with respect to the tape axis. As a result, the tapes in CORC® cables will retain close to 100% of I_c when wound at an angle of 45° as shown in figure 4, as long as the maximum strain does not exceed the irreversible strain limit under axial compression.

The method of winding a REBCO coated conductor at 45° on a round former allowed for a more precise determination of the irreversible strain limit under axial compressive strain of REBCO coated conductors and thus the minimum former size that could be used in CORC® cables. Because the reversible strain effect of I_c is negligible at this winding angle, any reduction in tape I_c after winding would be the result of mechanical degradation to the REBCO layer. Minimizing the former size increases the engineering current density in CORC® cables required for applications such as high-field magnets, resulting in a CORC® cable J_e of 344 A mm^{-2} at 17 T [26]. Figure 5(a) shows that REBCO tapes from SuperPower containing a substrate of 50 μm thickness retain their full I_c when wound onto a former as small as 4 mm thickness. Tapes with thinner substrates allow the use of formers of 3 mm (38 μm substrate) and 2.3 mm thickness (30 μm substrate) corresponding to about −1.2% axial strain in the REBCO layer (figure 5(b)). A minimum allowable former size of about 2.0 mm is expected for REBCO tapes with 25 μm thick substrates and of 1.6 mm for REBCO tapes with 20 μm thick substrates. Tapes with such thin substrates are expected to become available commercially from SuperPower Inc. in 2019 [27].

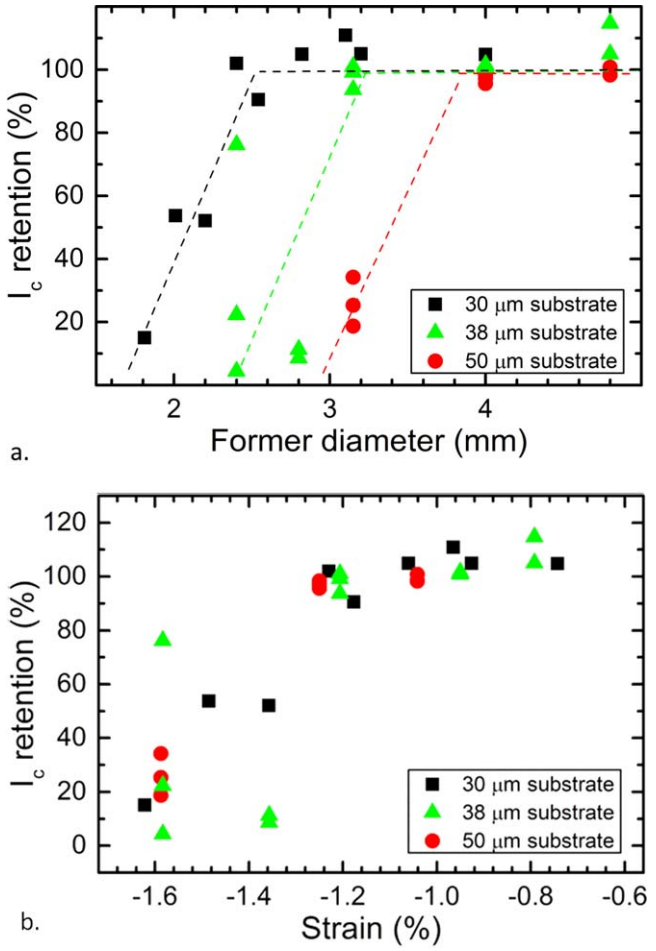

Figure 5. (a) Retention in critical current of IBAD-MOCVD REBCO tapes from SuperPower Inc. after winding the tapes on different size formers at an angle of 45°. (b) Retention of I_c as a function of maximum applied axial strain in the REBCO film.

2.2. CORC® cable and wire development at advanced conductor technologies

Advanced Conductor Technologies LLC [28] was founded in 2011 by Dr van der Laan after he invented the CORC® cable concept while at the National Institute of Standards and Technology (NIST) and the University of Colorado. The company goal is to develop the CORC® concept into a commercial product for use in the next generation of high-field magnets for fusion, particle accelerators and scientific applications, and for high-current density power cables for use in confined spaces such as Navy ships, electric aircraft and data centers.

The development of CORC® cables into a commercial product includes the ability to wind long CORC® cables with a custom winding machine (figure 6(a)). The machine allows winding of high-quality CORC® conductors in lengths exceeding 25 m with accurate control of winding tension and gap spacing between tapes. The machine is capable of winding 5–8 mm thick CORC® cables from 3–4 mm wide tapes containing 30–50 μm thick substrates and of winding 2.5–5 mm thick CORC® wires wound from 2–3 mm wide tapes containing substrates of 30 μm thickness. The

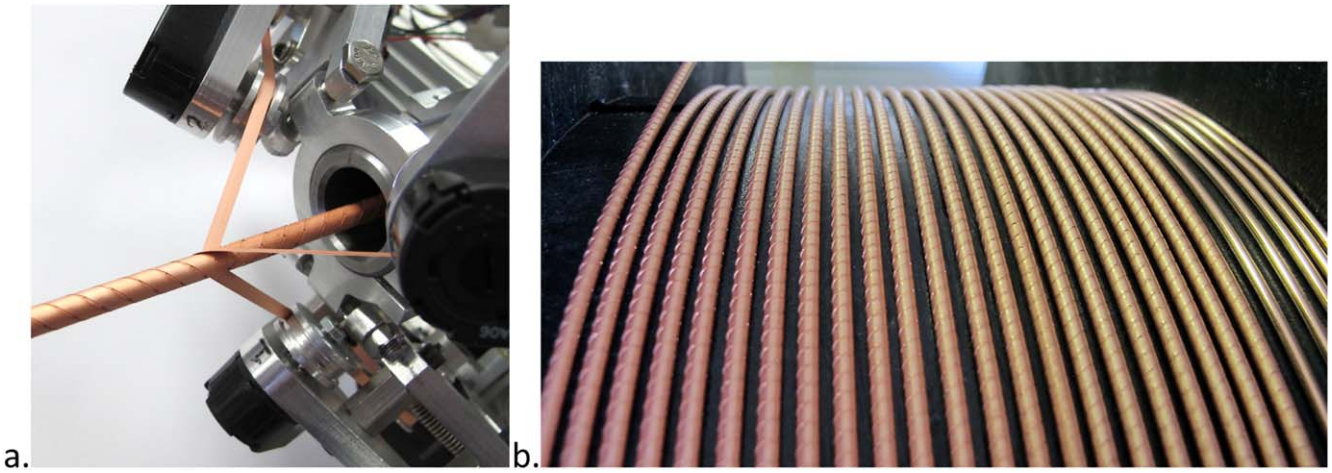

Figure 6. (a) Custom CORC® cable winding machine. (b) A 25 m long CORC® wire being wound.

Figure 7. A CORC® wire containing 16 tapes of 2 mm width, compared to a CORC® cable containing 30 tapes of 4 mm width.

introduction of commercial REBCO tapes with 30 μm thick substrates by SuperPower in 2016 [29] allowed Advanced Conductor Technologies to introduce the much thinner and more flexible CORC® wires [14] that were designed specifically for high-field magnet applications that require high J_e values and highly flexible conductors. Figure 7 shows a CORC® cable of 7 mm thickness and a CORC® wire of 3.2 mm thickness.

Several Phase I and Phase II Small Business Innovative Research and Small Business Technology Transfer programs awarded to Advanced Conductor Technologies since 2012 have led to a rapid development of CORC® cables and wires for various applications, some of which will be outlined in the following sections. The different programs have resulted in the development of multiple CORC® cable and wire configurations that were tested under various conditions, such as temperature, magnetic field, and mechanical stress. Table 1 shows an overview of several CORC® cables and wires that will be discussed in this article. The configurations listed in table 1 are a subset of the many possible conductor layouts to provide an overview of the technology and the many CORC® configurations that have been developed and characterized over the years. Many other configurations will be developed in the coming years when new tape geometries become available. The performance values listed in table 1 are calculated from a tape I_c at 76 K of 35 A mm^{-1} tape width, assuming no reduction in I_c due to cabling. The performance at 4.2 K and 20 T was calculated for two lift factors, defined as I_c(4.2 K, 20 T)/I_c(76 K, self-field), of 1.48 (typical) and 2.25 (record). Actual samples described in this paper contain tapes with a wide spread of tape I_c at 76 K and may contain tapes from different batches and thus different lift factors. Their performance could thus deviate significantly from the values listed in table 1.

2.3. Other REBCO cable approaches

2.3.1. Concentrically-wound REBCO power cables. Multi-tape REBCO cables were initially designed in an effort to increase the current capacity of REBCO tapes for application in the electric power grid. Two approaches were developed in parallel. The fist power cable approach was developed by ULTERA [1], initially using Bi-2223 tapes, and later using REBCO coated conductors. A round coaxial cable is formed by winding the tapes in a limited number of layers around a hollow tube through which sub-cooled liquid nitrogen is pumped. A three-phase ac cable is formed by winding each phase on top of one another, with a dielectric in between the phases (figure 8).

The second approach to cable REBCO coated conductors into a three-phase ac power cable consists of bundling three individual cables in which the REBCO tapes are wound in a limited number of layers onto a solid copper former [2]. Coolant flows around the bundle of three cables, that each contains a dielectric (figure 9). The limited cable flexibility is not a concern for use in long power cables that would replace existing cables in the power grid. These cables are unsuitable for use in high-field magnets, or in compact power cable systems due to their low current density and limited flexibility.

2.3.2. Twisted stacked tape cable. The most straightforward method to cable REBCO coated conductors into a high-

Table 1. Overview of CORC® cables and wires outlined in this article.

		CORC® C1	CORC® C2	CORC® C3	CORC® C4	CORC® W1	CORC® W2	CORC® W3	CORC® W4	CORC® W5	CORC® W6	CORC® W7	CORC® W8	CORC® W9
Type	—	Cable	Cable	Cable	Cable	Wire	Wire	Wire	Wire	Wire	Wire	Wire	Wire	Wire
Former size	(mm)	5.25	5.4	5.3	4.9	2.4	3.25	2.4	2.55	2.55	3.2	2.55	3.15	2.55
Tape number	—	24	30	42	9	12	12	16	27	29	28	50	18	30
Tape width	(mm)	4	4	4	4	2	3	2	2	2	3	2 + 3	2	2
Substrate thickness	(μm)	50	50	50	50	30	30	30	30	30	30	30	30	30
Number of layers	—	9	10	14	3	6	6	8	11	12	14	21	6	12
Outer diameter	(mm)	7.1	6.8	7.24	5.3	3	3.78	3.2	3.65	3.63	4.44	4.5	3.7	3.75
Cross-sectional area	(mm^2)	39.6	36.3	41.2	22.1	7.1	11.2	8.0	10.5	10.3	15.5	15.9	10.8	11.0
Hastelloy C-276 fraction[a]	—	0.18	0.25	0.31	0.12	0.15	0.14	0.18	0.23	0.25	0.24	0.35	0.15	0.24
Copper fraction[a]	—	0.69	0.68	0.60	0.88	0.69	0.79	0.62	0.57	0.58	0.60	0.44	0.78	0.54
I_c (76 K, s. f.)[b]	(A)	3360	4200	5880	1260	840	1260	1120	1890	2030	2940	4410	1260	2100
I_c (4.2 K, 20 T), LF = 1.48[c]	(A)	4973	6216	8702	1865	1243	1865	1658	2797	3004	4351	6527	1865	3108
J_e (4.2 K, 20 T), LF = 1.48[c]	($A\ mm^{-2}$)	126	171	211	85	176	166	206	267	290	281	410	173	281
I_c (4.2 K, 20 T), LF = 2.25[c]	(A)	7560	9450	13 230	2835	1890	2835	2520	4253	4568	6615	9923	2835	4725
J_e (4.2 K, 20 T), LF = 2.25[c]	($A\ mm^{-2}$)	191	260	321	129	267	253	313	406	441	427	624	264	428
Described in section	—	4.1	3.1.2	3.1.1 5.1	3.3.1	3.2.1	3.3.1 5.2	3.1.1 4.2/6	3.2.2 3.3.1	3.2.1 6	3.2.2	3.2.3	3.1.1 4.2	3.3.2
Performed measurement[d]	—	A	B	C, D	E	F	E, G	C, H, I	E, F	F, I	F	F	C, H	J

[a] With respect to total cross-sectional area.

[b] CORC® performance based on I_c of 35 A mm^{-1} tape width at 76 K and 100% I_c retention (no degradation due to cabling). s. f. = self-field.

[c] LF = lift factor defined as I_c(4.2 K, 20 T)/I_c(76 K, s. f.). Listed I_c and J_e values are maximum calculated values at 100% I_c retention based on select single tape measurements up to 14.5 T, extrapolated to 20 T.

[d] Measurements performed include:

A. Power cable test in helium gas.

B. Joint tests at 76 K and 4.2 K.

C. Termination tests at 76 K and 4.2 K.

D. SULTAN test at 4.2 K and between 10 and 60 K in helium gas up to 10.8 T.

E. Transverse compression testing at 76 K.

F. In-field testing at 4.2 K up to 12 T.

G. Testing of a multi-strand, sub-scale fusion cable at 76 K.

H. Fault current limiting wire testing at 76 K.

I. Testing of canted cosine-theta magnets at 77 K and 4.2 K.

J. Axial tensile stress testing at 76 K.

Figure 8. An HTS Triax® cable developed by ULTERA. © 2009 IEEE. Reprinted, with permission, from [3].

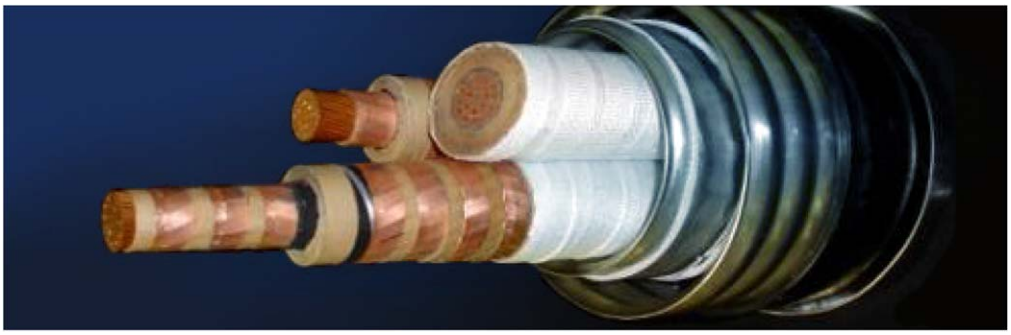

Figure 9. Three-phase ac cable installed as part of the grid in Albany, NY. Image provided by SuperPower Inc.

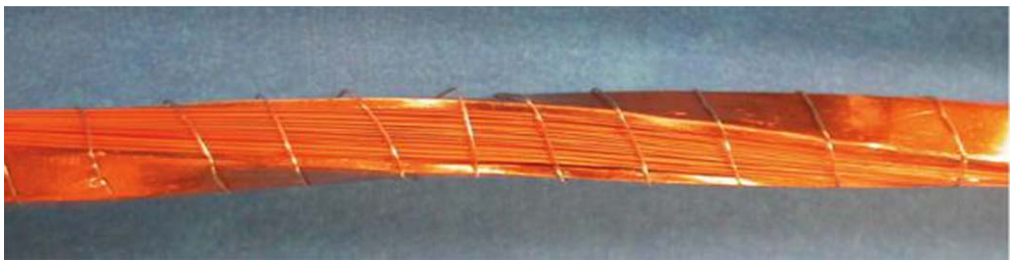

Figure 10. Overview of a bundle of REBCO tapes forming a TSTC. © 2013 IEEE. Reprinted, with permission, from [31].

current configuration was developed by MIT [30, 31]. The Twisted Stacked Tape Cable (TSTC) contains several coated conductors stacked on top of each other, after which the bundle is twisted (figure 10). The twist pitch allows for improved bending performance, while the overall current density in the stack is relatively high due to the absence of a former. Twisting the conductor results in the in-field performance of I_c that is determined by the magnetic field angle at which REBCO tapes experience the lowest I_c, which is perpendicular to the tape plane in case of 4.2 K operation. Twisting also results in a larger effective cross-section of the cable, compared to an untwisted stack, which lowers the engineering current density of the cable. The TSTC has been developed mainly for use in large magnet systems for fusion. Several fusion cable designs that incorporate one, or multiple stacks of REBCO tapes have been developed, including efforts at the Paul Scherrer Institute in Switzerland [32, 33], ENEA in Italy [34, 35], the CroCo cable design at Karlsruhe Institute of Technology in Germany [36, 37] and the STARS conductor at the National Institute for Fusion Science in Japan [38, 39]. The TSTC concept is also being explored to a limited degree for use in accelerator magnets [40] and other potential high-field applications using a stack of narrower, 1 mm wide REBCO tapes, such as the Twisted Soldered-Stacked-Square (3S) wire at Shanghai Jiao Tong University in China [41].

2.3.3. Roebel cable. The Roebel cable design was originally developed by Ludwig Roebel and patented in 1914 to provide a low-loss, high-current copper cable for use in large electrical machinery. The Roebel cable approach was first applied to REBCO tapes at the Karlsruhe Institute of Technology in 2006 [42] and at a later time produced commercially by Industrial Research Limited in New Zealand [43]. REBCO tapes are patterned (figure 11), after which the strands are assembled into a flat Roebel cable. The Roebel cable has a relatively high current density and contains fully transposed strands that results in a loss reduction under ac

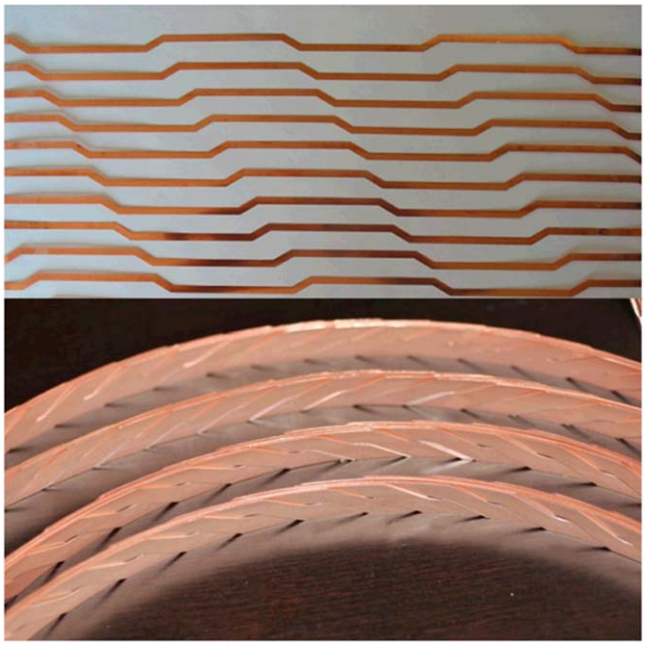

Figure 11. Patterned REBCO tapes before assembly into a Roebel cable (top). Overview of a REBCO-based Roebel cable (bottom). Reproduced from [44]. © IOP Publishing Ltd. All rights reserved.

operation and potentially a more homogeneous current distribution between strands during rapid current ramping. The Roebel cable is relatively flexible in one direction, but fairly inflexible when bent in plane, limiting the range of magnets suitable for Roebel cables. A large effort is underway at CERN to develop high-field accelerator magnets using Roebel cables [44, 45]. Several concepts of developing Roebel cables with higher operating current have been proposed in which several Roebel cables would be wound in parallel around a support structure, forming a Rutherford-type Roebel cable [46].

3. CORC® cable and wire performance

CORC® cables and wires are being developed into commercial conductors for use in a wide variety of applications, including high-field magnets, high-current power cables and magnet feeder cables. Each application comes with its own technical challenges, such as required conductor flexibility, minimum operating current and current density, tolerance to transverse compressive and axial tensile stresses, and their ability to withstand quenches resulting in rapid heating and cooling cycles. The following sections provide an overview of the current status of CORC® cable and wire performance and how continuous development keeps pushing the performance boundaries of these conductors. Unless stated otherwise, the performance of all samples was measured throughout the paper with voltage contacts located within the terminals. The voltage contacts thus span the entire CORC® cable or wire length and also measure the voltage coming from the contact resistance of the terminals. The critical current was determined at a criterion of 1 μV cm^{-1} with an uncertainty of 1%.

3.1. Current injection into CORC® cables and wires

Development of low-resistance terminations that enable homogeneous current injection into each of the tapes in the CORC® cable or wire has been one of the most important challenges during the initial development of CORC® conductors. An overview of the CORC® cable termination performance and of joints between cable terminations is provided next.

3.1.1. Terminating CORC® cables and wires. The large number of tape layers in CORC® cables and wires, ranging from six layers in a typical 12-tape CORC® wire, to over 20 in a 50-tape CORC® cable, presents a challenge for homogeneous current injection. The resistive buffer layers that insulate the REBCO layer from the metal substrate in REBCO coated conductors add to the challenge, because current can only be injected from the REBCO side of the tape, or through the thin copper layer that is often plated around the tape. Current injection from the CORC® terminal into each tape becomes inhomogeneous when the contact resistance between the tapes and the terminal varies significantly between tapes [47]. Inhomogeneous current distribution results in a nonlinear contact resistance as a function of current. Individual tapes may quench before other tapes reach I_c, resulting in a much lower cable I_c compared to that of the sum of all tapes.

Advanced Conductor Technologies developed a patented method to ensure all tapes in CORC® cables have a comparable contact resistance with the terminal, while keeping the terminals compact [48]. Terminating the CORC® cable involves trimming the REBCO tape layers at the cable ends, exposing the tapes in each layer. Since the tapes are wound onto a small former, and their substrate remains partly elastic, the REBCO tapes have the tendency to expand radially outward when released after trimming (see figures 7 and 12), allowing them to come into direct contact with the copper tube that is placed over the cable end and forms the terminal. Electrical contact is made between the tapes and the tube by filling the tube with solder.

Micrographs of the longitudinal cross-section of a CORC® cable termination, taken at two different locations along its length, clearly demonstrate the radial expansion of the REBCO tapes in the terminal (figure 13). The outer diameter of the terminal is somewhat larger than that of the CORC® cable or wire, and is about 12.6 mm for an 8 mm thick CORC® cable, and 6.3 mm for a 3.6 mm CORC® wire (figure 14).

The resistivity of the solder used to fill the CORC® cable terminals has a large impact on their overall contact resistance, because current flows partly through the solder to circumvent the resistive buffer layer that separates the REBCO layer from the copper tube. The difference in electric field (E) versus current and overall contact resistance of a 16-tape CORC® wire (CORC®-W3 in table 1) was determined at

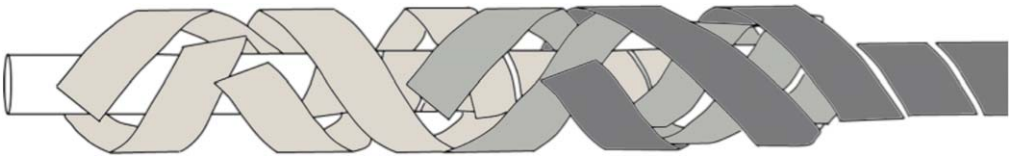

Figure 12. Tapered end of a CORC® cable in which the tapes expand radially and come into direct contact with the copper terminal (not shown).

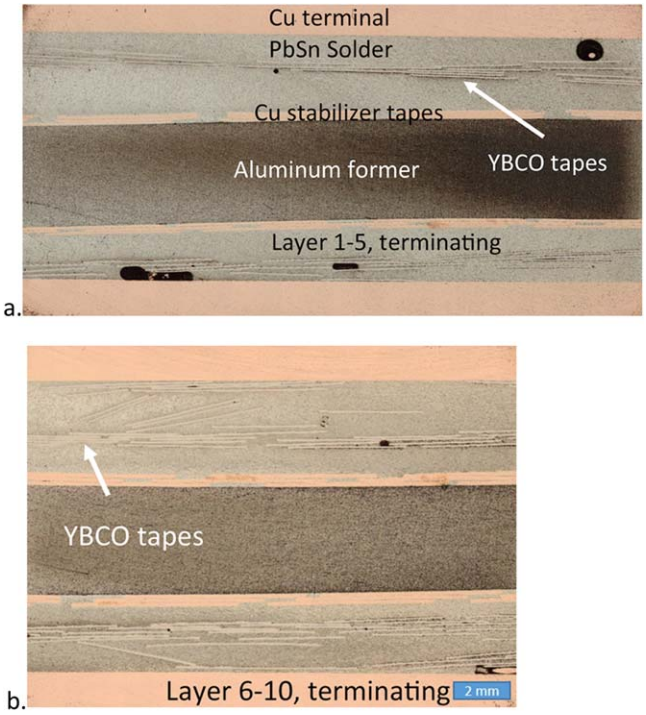

Figure 13. Micrograph of the longitudinal cross-section of a CORC® cable terminal, (a) near the end of the terminal, and (b) where the cable enters the terminal. Layers are counted from the former outward.

76 K for terminals filled with 63Sn–37Pb solder, and for terminals filled with 100In solder (figure 15(a)). In both cases, the terminals were 15 cm in length and each of the eight layers in the CORC® wire was tapered. The voltage contacts were located about halfway into the terminal, between the copper tube and the bundle of tapes. The lower resistivity of 100In solder resulted in a significant reduction in contact resistance (16.2 nΩ) compared to terminals in which 63Sn–37Pb solder was used (142 nΩ). The use of 100In solder also resulted in a much sharper superconducting transition at a critical current of 652 A and n-value of 13, compared to an I_c of 546 A, and an n-value of only 5 when using 63Sn–37Pb solder. A second CORC® wire (CORC®-W8 in table 1) containing 100In filled terminals showed no significant change in performance when it was measured again after 4 and 11 months (figure 15(b)), indicating that potential alloying at room temperature between the indium solder and the copper plating of the tapes over that timeframe did not influence their performance.

The method of terminating CORC® cables and wires in a tube after the tape layers have been trimmed remains effective even when the CORC® cable or wire contains a high number of tapes, such as sample CORC®-W5 (table 1) with 29 tapes wound into 12 layers and sample CORC®-C3 containing 42 tapes wound into 14 layers. At 76 K, the CORC® wire I_c was 2191 A, and the contact resistance 24.9 nΩ, while I_c of the CORC® cable was 4233 A, and its contact resistance was about 26 nΩ (figure 16(a)). A second sample of CORC®-W5 was also prepared for in-field measurements by winding a length of the CORC® wire into a five-turn coil around a 60 mm mandrel [49]. The V–I characteristics at 76 K in self-field and at 4.2 K in a background field of 10 T are shown in figure 16(b). The I_c of the wire at 76 K was about 1500 A, due to the significant self-field that the five-turn coil produced, and the contact resistance was 35.9 nΩ. At 4.2 K and 10 T, the contact resistance of the terminals, which were located in a stray field of about 3 T, was 4.11 nΩ, while the wire I_c was about 4000 A. The contact resistance of the 100In filled terminals was thus reduced by a factor of 8.75 when it was cooled down from 76 to 4.2 K.

The results of measurements in self-field at 76 K of CORC® cables and wires show that the optimized terminations indeed allow for a low and constant contact resistance and a sharp superconducting transition at currents close to the total I_c of the tapes. This is an indication of current being injected homogeneously into each tape, which clears an important hurdle for CORC® cables and wires to become a viable solution for many high-field and power cable applications.

3.1.2. Joints between CORC® cable terminals. One significant challenge in determining the actual contact resistance of a CORC® cable terminal is where to measure the voltage between the terminal and cable. In most cases, current is injected radially from copper adapters that are clamped onto the round terminals, and several pairs of voltage contacts that are embedded in the solder between the copper terminal and the cable within the terminal. These voltage contacts measure the majority of the voltage generated when injecting current into the cable, although variations in their precise location may cause uncertainty in determining the exact contact resistance.

A more precise method to determine the contact resistance of CORC® terminals, and the effect of trimming the tape layers at the cable ends, is by preparing a CORC® cable joint. The joint is inserted into a CORC® cable that contains a pair of terminations with voltage contacts at both cable ends. Any change in resistance measured with these voltage contacts after the joint has been inserted thus originates from the joint.

Figure 14. Tube terminations mounted on a CORC® cable (top) and a CORC® wire (bottom).

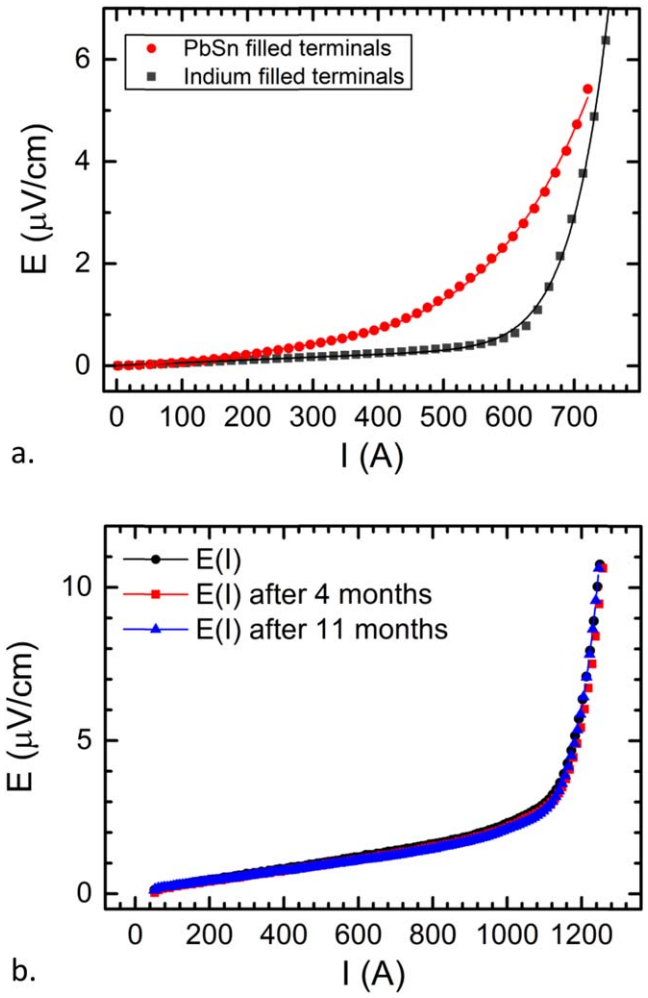

Figure 15. (a) Comparison of the electric field versus current characteristics of two 16-tape CORC® wires (CORC®-W3) containing terminals filled with 63Sn–37Pb solder and 100In solder. (b) *E–I* measurements of a CORC® wire (CORC®-W8) with 100In filled terminals performed 11 months apart. The solid lines are a fit to the data. Data taken at 76 K.

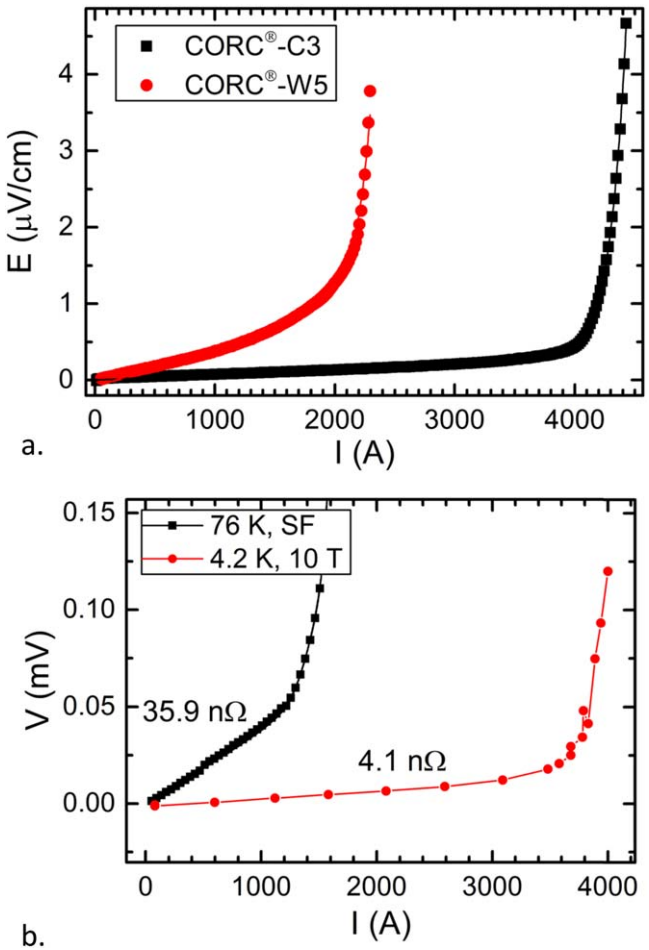

Figure 16. (a) *E–I* characteristics measured at 76 K of a 29-tape CORC® wire (CORC®-W5) and a 42-tape CORC® cable (CORC®-C3). (b) *V–I* characteristics of a sample CORC®-W5 measured at 76 K in self-field and of the same wire at 4.2 K in a magnetic field of 10 T and after being wound into a five-turn coil of 60 mm inner diameter. The CORC® wire length and thus the separation between voltage contacts was about 1.5 m.

Figure 17(a) shows the copper structure with which a CORC® cable joint was made. The joint was formed by a rectangular copper bar containing two round channels into which the two CORC® cable ends were terminated. Such structure removes any contact resistance associated with pressure contacts between separate terminals that may form a joint. Figure 17(b) shows a CORC® cable joint (CORC®-C2 in table 1) with the original end terminals 15 cm in length mounted within the copper adapters used to inject current. The terminals and the joint were filled with 100In solder. The contact resistance of the terminals, measured with the pair of voltage contacts located within the two end terminals, was 60 nΩ at 76 K. This value formed the baseline resistance associated with these injection terminals (figure 18(a)).

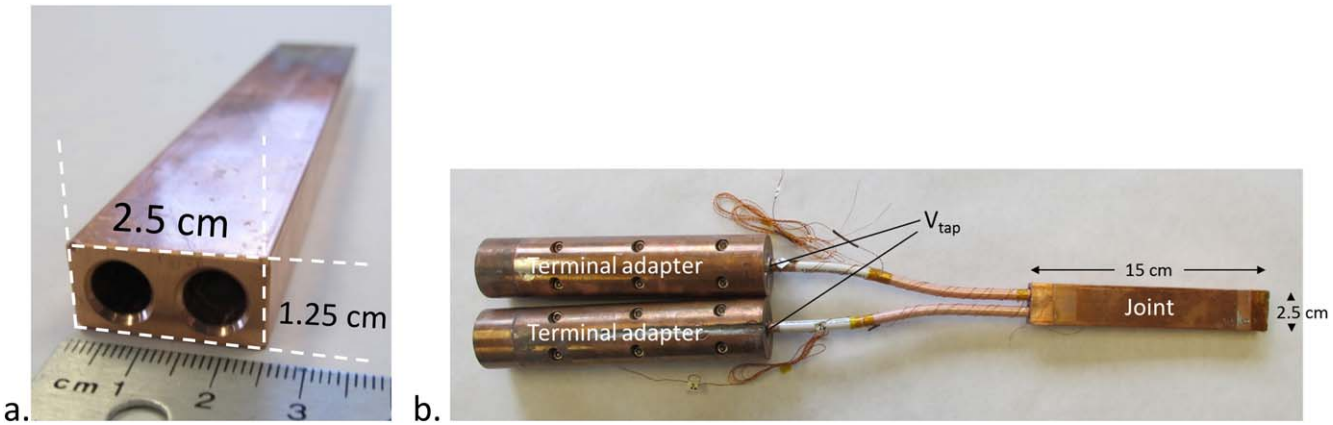

Figure 17. (a) Copper joint structure into which the two CORC® cable ends were terminated to form a joint. (b) The sample showing copper adapters on the left that inject current into the cable terminals that contain voltage contacts, and the joint (right) formed by soldering the CORC® cable ends into the copper joint structure.

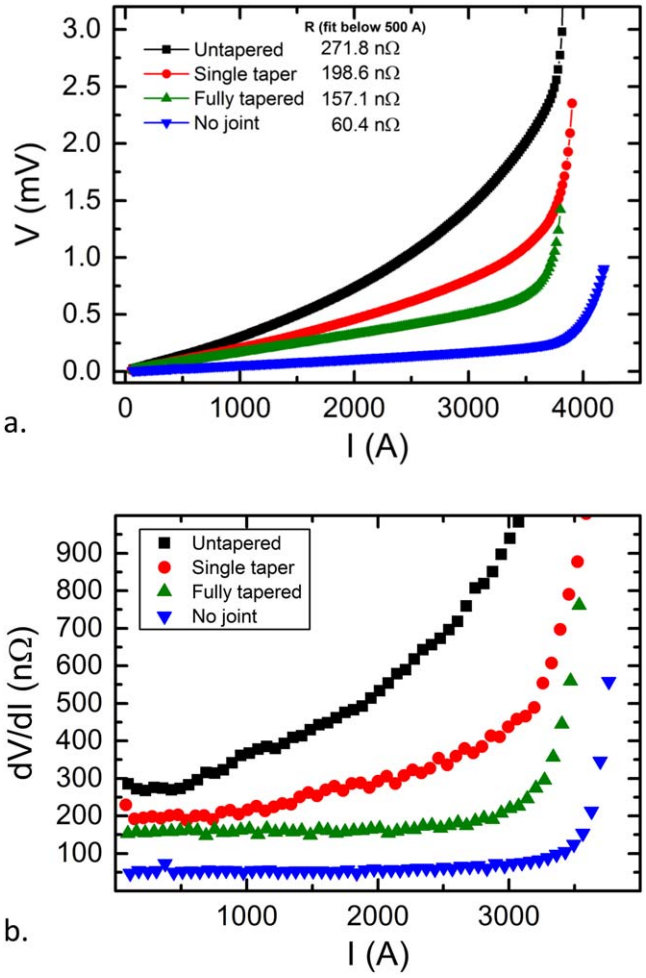

Figure 18. (a) *V–I* characteristics of the various joints measured at 76 K. (b) The first derivative of the total voltage as a function of current.

The derivative of the *V–I* curve measured over the cable before a joint was inserted was constant up to a current of close to 3500 A, at which point the superconducting transition started (figure 18(b)). The cable I_c was 4032 A, or 80% of the total I_c of the tapes in the cable, with an *n*-value of over 25. The contact resistance of the first joint that was inserted, and did not contain any tapered layers of the CORC® cable, was between 229 and 1177 nΩ after subtracting 60 nΩ associated with the injection terminals, depending on the current range over which the contact resistance was calculated (see table 2). The critical current decreased by about 15% compared to the CORC® cable I_c before the joint was inserted, due to the higher self-field on the cables coming from the joint. The contact resistance was reduced to between 138 and 440 nΩ after the joint was replaced with one that contained a single taper and to 97 nΩ for a joint in which each tape layer in the CORC® cable was tapered. The derivative of the voltage was highly dependent on current for joints in which the cables were not tapered, or contained only a single taper, indicating a highly inhomogeneous current injection into the cable. Only the joint in which all tape layers were tapered showed no sign of inhomogeneous current injection. Dissipation in the joint at a current of 3000 A decreased from about 4.5 W for the non-tapered joint to only 0.87 W for the fully tapered joint.

The samples containing un-tapered and the fully tapered joints were also measured in self-field at 4.2 K in liquid helium. The measurement shows a linear *V–I* curve for both samples up to the maximum testing current available of 9000 A (figure 19), which is expected to be about 20%–30% of the self-field I_c at 4.2 K. The contact resistance of the joint and the injection terminals was 14.9 nΩ for the un-tapered joint, and 9.8 nΩ for the fully tapered joint. The original cable length of 2 m prevented us from measuring its performance at 4.2 K before a joint was inserted, due to space limitations. A direct baseline contact resistance of the injection terminals at 4.2 K could therefore not be obtained. On the other hand, the ratio between the contact resistance of the injection terminals and the joint is expected to remain the same. This would suggest the contact resistance at 4.2 K of the un-tapered joint to be 11.6 nΩ and that of the fully tapered joint to be 6 nΩ. The contact resistance thus decreased by a factor of 15–20 when cooled from 76 to 4.2 K. The contact resistance could potentially be decreased further by increasing the length of the joint.

Table 2. Performance of the various joints measured at 76 K.

		No joint	Un-tapered	One taper	Fully tapered
I_c (76 K)	(A)	4032	3400–3800	3499	3465
n-value	—	25	NA	18	29
Total *R*	(nΩ)	60	289–1237	199–500	157
Joint *R*	(nΩ)	NA	229–1177	138–439.6	97
Dissipation (3 kA)	(W)	NA	4.5	2.25	0.87

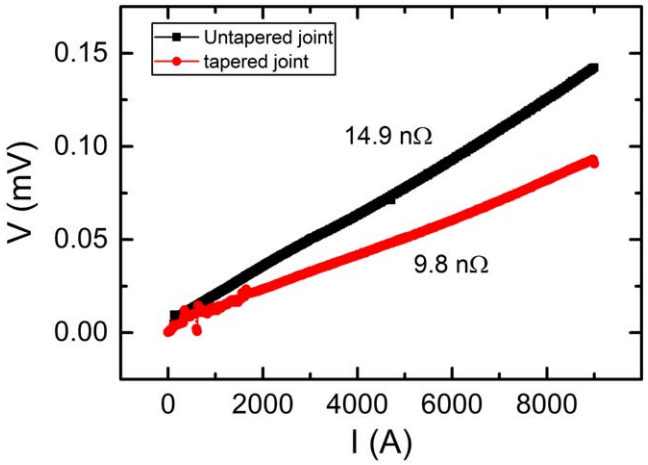

Figure 19. *V–I* curves to about 20%–30% of the CORC® cable I_c of the joint with no taper and a fully tapered joint, measured at 4.2 K in self-field.

3.2. CORC® cable and wire performance at high magnetic fields

CORC® cables and wires are being developed for a variety of high-field magnet applications, including fusion machines, particle accelerators, and scientific research magnets. High-field magnets come with some of the most stringent requirements for any HTS cable. Fusion magnets may require operating currents of between 50 and 100 kA in background fields of 10–20 T, while particle accelerator magnets may require operating currents of 10–20 kA in a background field exceeding 20 T, while having a current density based on the cable cross-section of at least 300 A mm^{-2}, and preferably exceeding 600 A mm^{-2}.

The in-field performance of CORC® cables or wires is fully isotropic with respect to magnetic field angle and at 4.2 K closely follows the magnetic field dependence of I_c of the tapes for field applied perpendicular to the tape surface [50]. First order estimates of the CORC® cable in-field performance at 4.2 K can thus be made based on the individual tape performance. Such estimates do not take into account any potential I_c reduction due to cabling, cable bending, inhomogeneous current injection, or degradation due to high mechanical stresses that act on the conductor when operated at high current in a background magnetic field. Actual performance tests of CORC® cables and wires in magnetic fields of 10–20 T are thus required as part of their successful development.

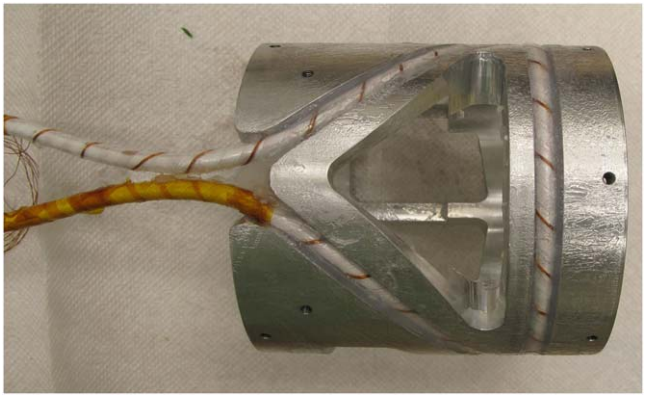

Figure 20. CORC® cable wound onto a 100 mm diameter sample holder, designed to fit into the since-decommissioned Large Bore Resistive Magnet at the NHMFL and in the 8.75 T superconducting magnet at the University of Colorado.

3.2.1. Magnet facilities in which CORC® cables and wires have been tested. The main facility in which CORC® cables were tested between 2011 and 2015 was the Large Bore Resistive Magnet Facility at the National High Magnetic Field Laboratory (NHMFL) in Tallahassee, Florida. The resistive Bitter magnet with 195 mm diameter warm bore generated a magnetic field of 19.8 T, but degraded to 19 T in 2012 and to 17 T in 2014. The large magnet bore allowed for testing of CORC® cables wound onto a 100 mm diameter sample holder (figure 20) although, at the time, this diameter was close to the limit to which CORC® cables could be bent. Several performance records of high-current CORC® cables were reached in this facility.

CORC® cables first exceeded a J_e(20 T) of 100 A mm^{-2} at a critical current of almost 5 kA in 2012 [50]. This record was broken in 2014 when a 6 mm thick, 50-tape CORC® cable wound from tapes containing 38 μm thick substrates was tested in fields up to 17 T. The performance, extrapolated to 20 T, predicted a J_e of 217 A mm^{-2} at a cable I_c of over 6 kA [51]. The final measurement before the facility was decommissioned in October 2015 resulted in yet another record CORC® cable performance of J_e(20 T) = 309 A mm^{-2} in a 5.1 mm thick CORC® cable wound from 50 tapes containing substrates of 30 μm thickness [26]. An overview of the CORC® cable J_e extrapolated to 20 T as a function of date when the measurements were performed is shown in figure 21.

CORC® cable testing at high magnetic fields was suspended after the magnet at the NHMFL was decommissioned, because no other high-field magnet was available in the US in which CORC® cables could be tested when bent to

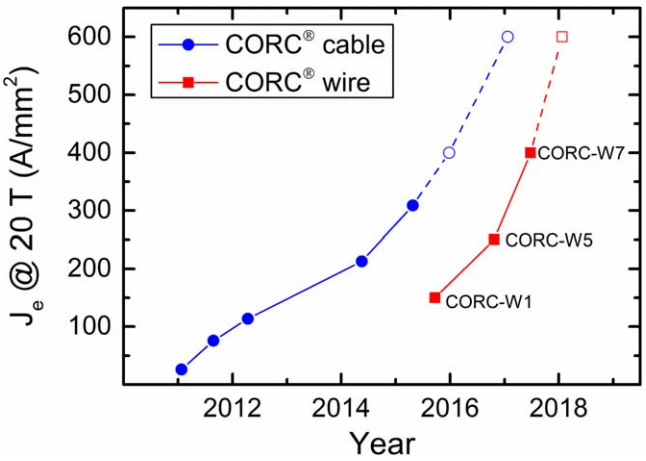

Figure 21. Engineering current density at 4.2 K, extrapolated to a magnetic field of 20 T, in CORC® cables and wires as a function of measurement date. The open symbols are J_e projections. The CORC® cables were measured on a sample holder of 100 mm diameter in the Large Bore Resistive Magnet at the NHMFL, while the CORC® wires were measured on a sample holder of 60 mm diameter at the University of Twente (2016) and at the University of Colorado (2017).

100 mm diameter. Although an 8.75 T superconducting magnet with large enough bore to fit the probe was available at the NIST (figure 22), its relatively low magnetic field would result in a CORC® cable I_c of more than 16 kA that would exceed the limits of the available power supplies and current leads.

Only after the introduction of much more flexible CORC® wires in 2016, wound from 2 and 3 mm wide tapes containing substrates of 30 μm thickness, did in-field testing of CORC® conductors resume. The high flexibility of CORC® wires allowed winding on a 60 mm diameter sample holder (figure 23), small enough to fit in superconducting magnets with 80 mm cold bores, such as a 10 T magnet at the University of Twente and a 12 T magnet at the University of Colorado. The first CORC® wire containing 12 tapes of 2 mm width (CORC®-W1 in table 1) was measured at the University of Twente using a superconducting transformer, where it reached an I_c of 1600 A at 10 T, and an extrapolated J_e(20 T) of 114 A mm^{-2} [14], followed by a second CORC® wire containing 29 tapes (CORC®-W5 in table 1) that reached an extrapolated J_e(20 T) of 250 A mm^{-2} in 2017 [49].

The much smaller size of CORC® wires that allowed bending to smaller diameters also results in lower critical currents and lower J_e-values at 20 T, compared to the CORC® cables that were tested just before the magnet at the NHMFL was decommissioned. Their much higher flexibility makes CORC® wires more suitable for use in accelerator magnets that require tighter conductor bends that cannot be achieved with CORC® cables. Further development of the CORC® wires to allow even tighter bends in combination with higher in-field performance is underway. Some of the latest, previously unpublished, results will be outlined in the following sections.

3.2.2. Development of CORC® wires for use in accelerator magnets. Several CORC® wires were tested in the 12 T superconducting magnet at the University of Colorado (transferred from NIST in 2016) using external power supplies instead of a superconducting transformer. The test results of two CORC® wires are outlined in this section, one containing 27 tapes of 2 mm width (CORC®-W4 in table 1), and one containing 28 tapes of 3 mm width (CORC®-W6). The test results are compared to the in-field performance of the individual tapes, measured by our collaborators at the Applied Superconductivity Center (ASC) at the NHMFL, from which the CORC® wires were wound.

Both CORC® wires were tested in liquid nitrogen at 76 K before they were wound onto the 60 mm diameter sample holder. Sample CORC®-W4 had an I_c of 1644 A (figure 24(a)), while sample CORC®-W6 had an I_c of 2831 A (figure 24(b)). Both samples had an I_c of about 80% of the combined tape I_c. The I_c reduction is likely a consequence of the self-field generated by the sample, especially in its terminals, and the varying strain of tapes wound at winding angles of more or less than 45° (see section 2.1). The critical current of sample CORC®-W6 was also measured at 76 K after it was wound onto the sample holder and supported by Stycast 2850 epoxy (figure 25), where I_c was 2281 A due to the relatively high self-field generated by the sample loop.

The *V–I* curves of sample CORC®-W4, measured at 4.2 K in fields between 5 and 12 T, and of sample CORC®-W6 for fields between 6 and 11 T are shown in figure 26. The voltage was measured over the sample terminals and thus includes their contact resistance. Current in sample CORC®-W4 was increased until the sample quenched, while a quench detector switched off the sample current once the voltage exceeded 3 mV. The first measurement was performed at 12 T, with the sample current polarity such that the self-field of the sample added to the external field and the Lorenz force was directed outward. The current was cycled between 0 and 90% of the quench current a total of 55 times to stress cycle the sample at a Hoop stress of about 110 MPa, after which the full *V-I* curve was measured again. No significant difference in performance was measured, demonstrating that the sample did not degrade. The critical current was 3835 A at 12 T (table 3) and 6802 A at 5 T. Sample CORC®-W6 could only be measured down to a magnetic field of 6 T due to its higher critical current of 9276 A (table 4). The data listed in tables 3 and 4 include the applied magnetic field and the total magnetic field, which is the sum of the applied field and the field generated by the sample. The self-field on the magnet axis was calculated from the current of the small sample coil wound onto the 60 mm diameter mandrel. The high I_c of sample CORC®-W6 at an applied field of 6 T resulted in a self-field of almost 1.2 T.

Figure 27 shows the magnetic field dependence of I_c of samples CORC®-W4 and CORC®-W6, including the sum of their tape critical currents. The self-field of the samples was taken into account. The magnetic field dependence at high

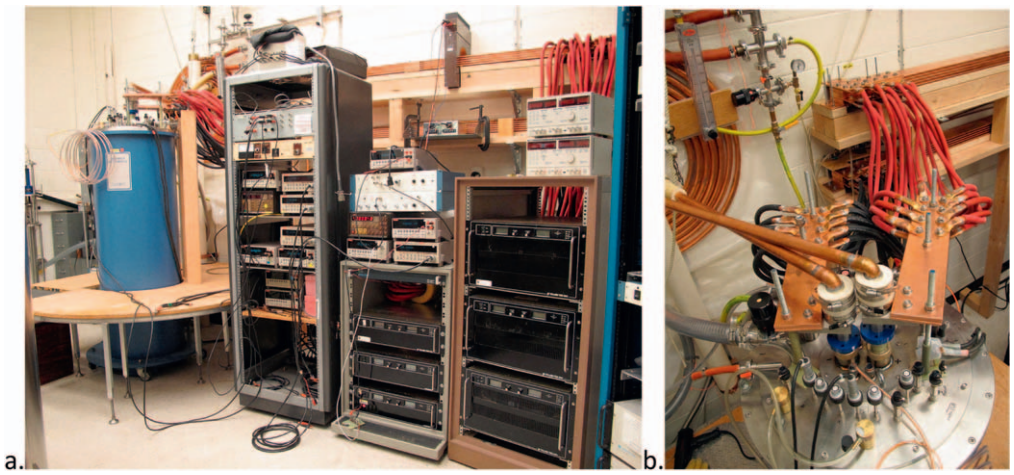

Figure 22. (a) Superconducting 8.75/12 T magnet with power supplies at the NIST, which was transferred to the University of Colorado in 2016. (b) Current bus-bars and vapor-cooled current leads capable of injecting 16 kA of current into CORC® wires when tested in the magnet.

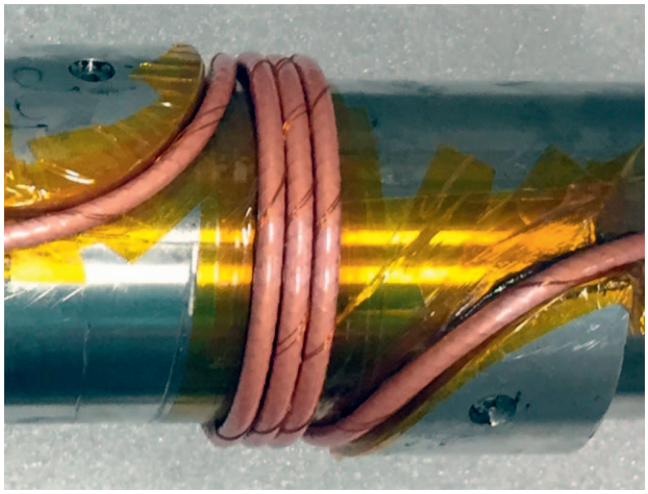

Figure 23. CORC® wire wound around the 60 mm diameter insert for measurements in the 80 mm diameter bore 10 T magnet at the University of Twente. © 2018 IEEE. Reprinted, with permission, from [49].

field was fitted with the following power law function:

$$I_c(B) = I_c(0)B^{-\alpha}, \tag{4}$$

where $I_c(0)$ is the critical current in self-field and α is the slope of the $I_c(B)$ dependence in a double-logarithmic plot. The tape I_c measurements performed at fields up to 15 T at the ASC-NHMFL showed that the high-field pinning in the 2 mm wide tapes was relatively low, resulting in an expected I_c at 12 T of 5139 A. In fact, the lift factor of sample CORC®-W4 at 12 T, defined as $I_c(4.2\,\text{K},12\,\text{T})/I_c(76\,\text{K}$, self-field), was about 2.3, while values exceeding 2.5–3 are more typical [26].

At high field, sample CORC®-W4 had an I_c of about 75.7% of the total expected tape I_c. The deviation could come from actual degradation in the CORC® wire performance that is the result of winding the sample on the small sample holder. It could also be caused by variations in actual tape performance, with respect to I_c and pinning, that were not visible within the very limited number of tapes that were measured at high field. Yet another explanation is that I_c of the inner tapes degraded because the former size was close to

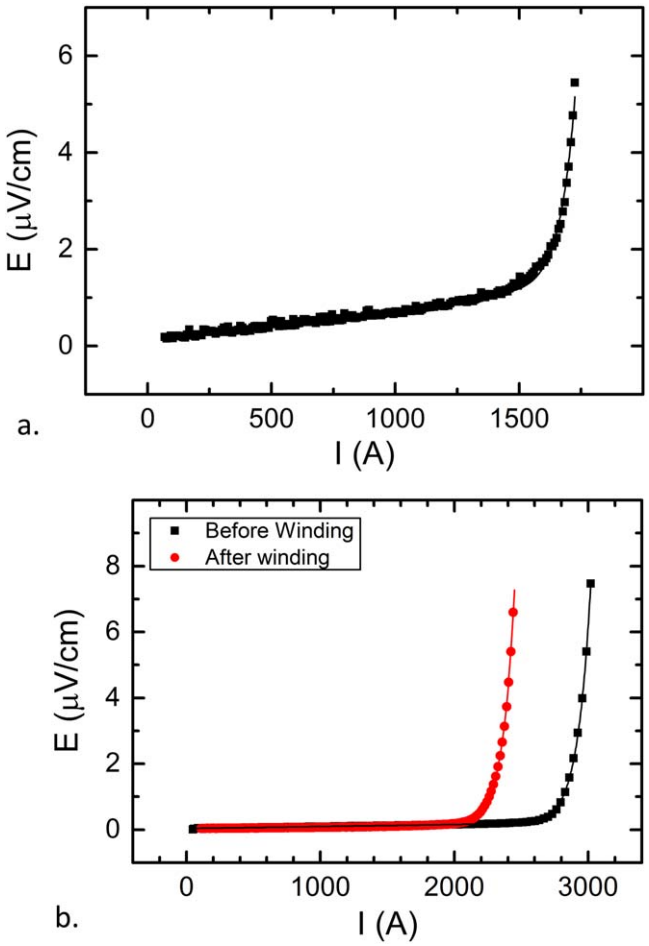

Figure 24. *E–I* characteristic measured at 76 K of (a) sample CORC®-W4 before winding, and (b) sample CORC®-W6 before and after winding onto the 60 mm diameter sample holder. The lines are a fit to the data.

the critical size at which the REBCO layers experience −1.25% axial strain. The CORC® wire I_c at 20 T would be about 2648 A, based on extrapolation of the field dependence of I_c, resulting in a $J_e(20\,\text{T})$ of 259 A mm^{-2}.

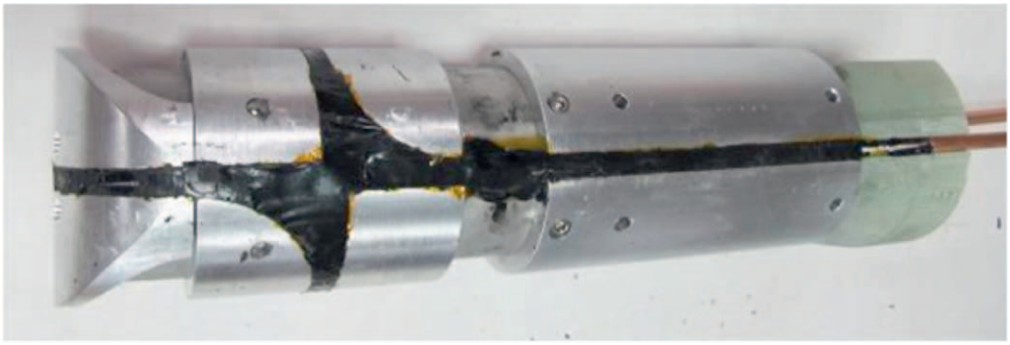

Figure 25. Sample CORC®-W4 wound onto the sample probe and embedded in Stycast 2850 epoxy for testing in high magnetic fields.

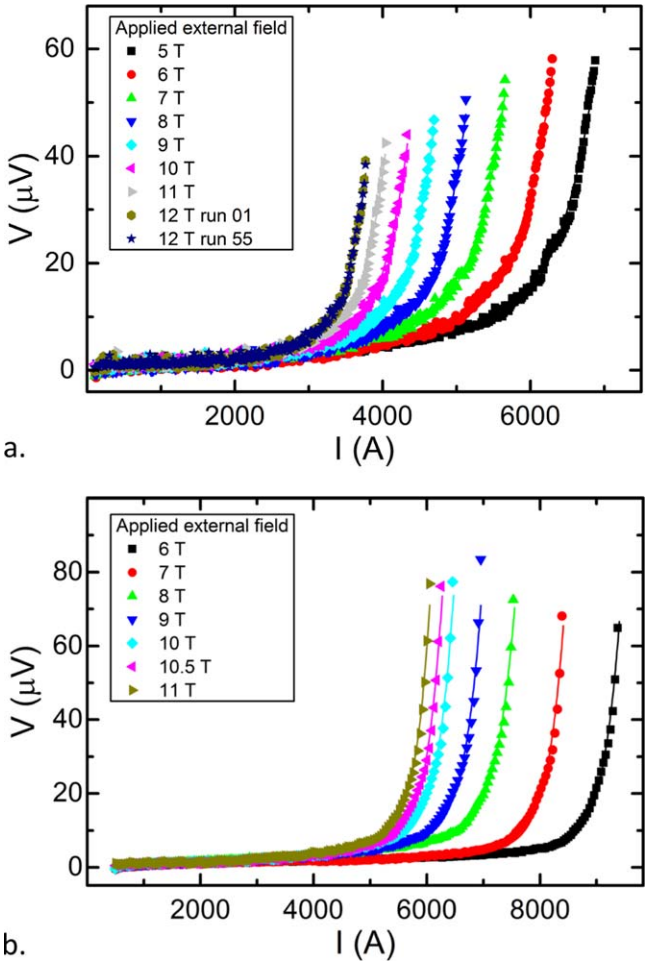

Figure 26. (a) *V–I* curves of CORC®-W4 measured at 4.2 K at applied magnetic fields between 5 and 12 T. (b) *V–I* curves of CORC®-W6 measured at 4.2 K at applied magnetic fields between 6 and 11 T.

Table 3. Performance of CORC®-W4 at high magnetic fields at 4.2 K.

B (T)	B + s. f. (T)	I_{quench} (A)	I_c (A)	n-value (-)
1	1.68		10 525	4
2	2.61	9700	9394	6
3	3.54	8543	8350	8
4	4.49	7730	7492	12
5	5.44	7005	6802	14
6	6.4	6365	6216	13
7	7.36	5723	5619	13
8	8.33	5193	5119	13
9	9.31	4736	4708	13
10	10.28	4390	4363	13
11	11.26	4091	4076	13
12	12.25	3835	3831	13

Table 4. Performance of sample CORC®-W6 at high magnetic fields at 4.2 K.

B (T)	B + s. f. (T)	I_c (A)	n-value (-)
6	7.19	9276	31
7	8.08	8293	29
8	8.97	7403	23
9	9.9	6820	23
10	10.84	6333	23
10.5	11.32	6137	23
11	11.79	5932	23

The 3 mm wide tapes from which sample CORC®-W6 was wound had even worse pinning, with a lift factor at 12 T of only 2. The I_c retention of the 3 mm wide tapes was about 86%, which was higher than that of sample CORC®-W4, likely because the slightly larger former of 3.2 mm provided the inner tapes with a larger strain margin. The projected J_e at 20 T of sample CORC®-W6 was 247 A mm^{-2}. The engineering current densities obtained in the two CORC® wires already come close to the minimum practical J_e value of 300 A mm^{-2} that is often mentioned for future accelerator magnets and about halfway to the ultimate goal of 600 A mm^{-2} at 20 T. Both CORC® wires already have a higher J_e at 10 T than reported for Roebel cables in perpendicular magnetic field; between 430 and 400 A mm^{-2} for both CORC® wires, compared to 364 A mm^{-2} for Roebel cables [52, 53].

3.2.3. Record current density in CORC® wires at 20 T. A high tape count CORC® wire (CORC®-W7 in table 1) was prepared from a total of 50 tapes of 2 and 3 mm width, containing 30 μm substrate, in an effort to reach a J_e at 20 T that would exceed the highest J_e(20 T) of 309 A mm^{-2} reached in a CORC® cable bent to 100 mm diameter [26]. The CORC® wire was wound from tapes with relatively high lift

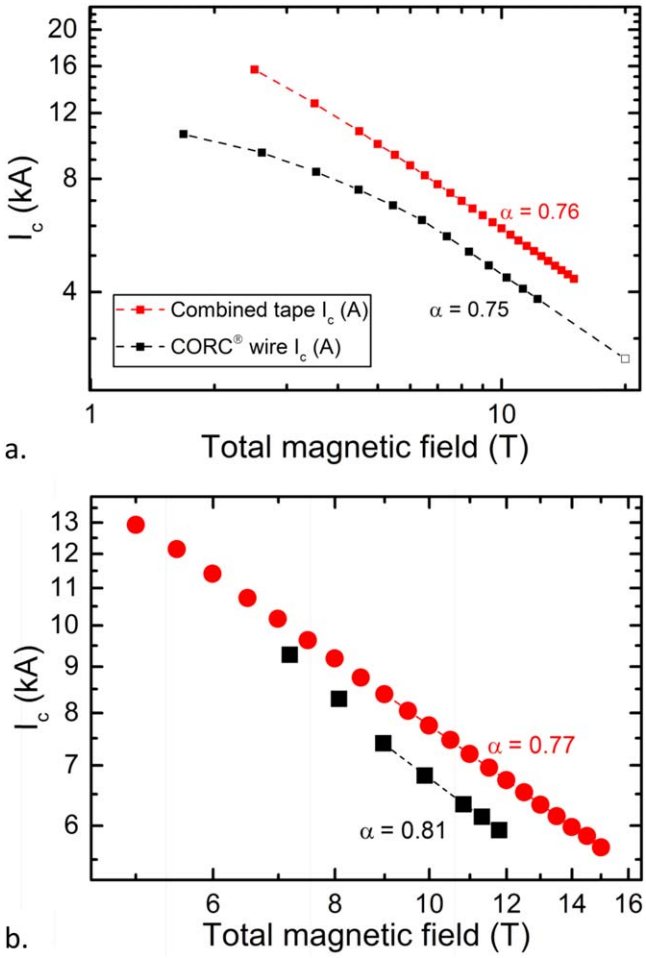

Figure 27. Magnetic field dependence at 4.2 K of the combined tape I_c and the CORC® wire I_c (a) of sample CORC®-W4, and (b) of sample CORC®-W6. The fits using the power-law dependence according to equation (4) are included. The magnetic field includes the self-field of the sample.

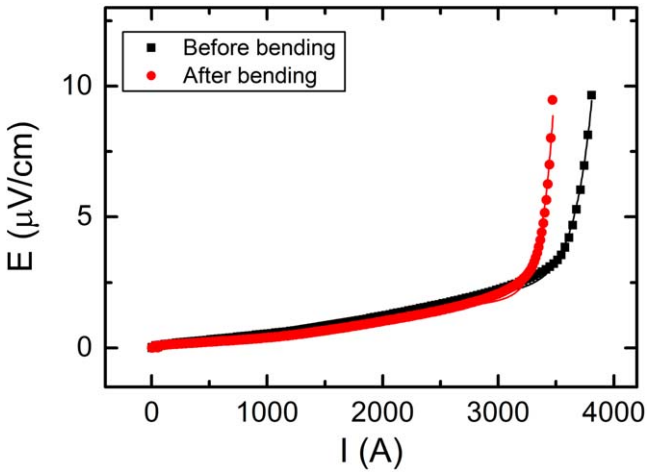

Figure 28. *E–I* characteristic of the high-J_e sample CORC®-W7, measured in liquid nitrogen at 76 K before and after bending into the 60 mm diameter hairpin. The lines are fits to the data.

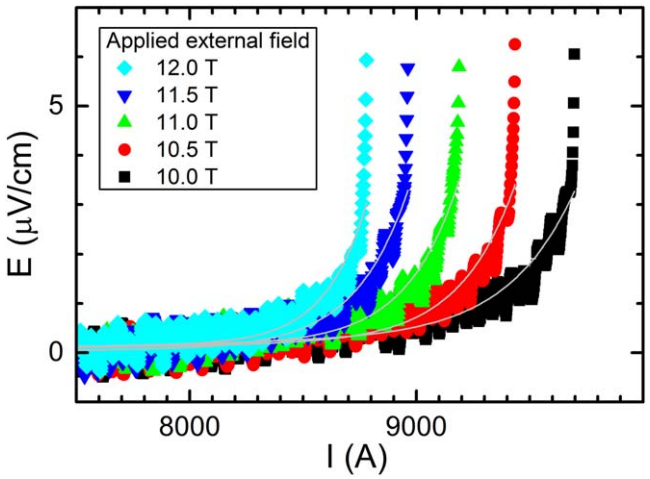

Figure 29. *E–I* curves of the high-performance sample CORC®-W7, measured at 4.2 K at magnetic fields between 10 and 12 T. The solid lines are fits to the data.

factors of 3–3.4 at 4.2 K and 12 T, much higher than those used in samples CORC®-W4 and W6. Figure 28 shows the *E–I* characteristics of sample CORC®-W7 measured at 76 K before and after being bent into a 60 mm diameter hairpin. The critical current decreased from 3522 to 3282 A after bending into the hairpin, most likely because of increased self-field.

The *E–I* curves of sample CORC®-W7 were measured at fields between 10 and 12 T (figure 29). At 12 T, the sample had a quench current of 8813 A and an I_c of 8591 A (table 5). Measurements below 10 T could not be performed because of the high CORC® wire current. The *E–I* curves were very steep and the sample would quench at a current only slightly above I_c. The measurements were repeated several times at each field, confirming that the *E–I* curves did not change and that the sample did not degrade after each quench.

The magnetic field dependence of I_c of sample CORC®-W4 as a function of magnetic field is shown in figure 30, including that of the total tape I_c. The tape I_c, measured up to 14.5 T was fitted with equation (4) using a value of 0.78 for α, while $\alpha = 0.51$ was used for the CORC®

Table 5. Performance of sample CORC®-W7 at high magnetic fields at 4.2 K.

B (T)	I_{quench} (A)	I_c (A)	n-value (-)
9	10 239		
10	9710	9390	33
10.5	9461	9157	39
11	9206	8924	41
11.5	8995	8694	38
12	8813	8591	48
20		6601[a]	

[a] Extrapolated value.

wire I_c. The extrapolated CORC® wire I_c at 20 T would be 6601 A, resulting in an extrapolated J_e at 20 T of 423 A mm^{-2}, which is a new record for CORC® conductors. The CORC® wire I_c was about 71.8% of the total tape I_c, although this is based on a very limited number of tape

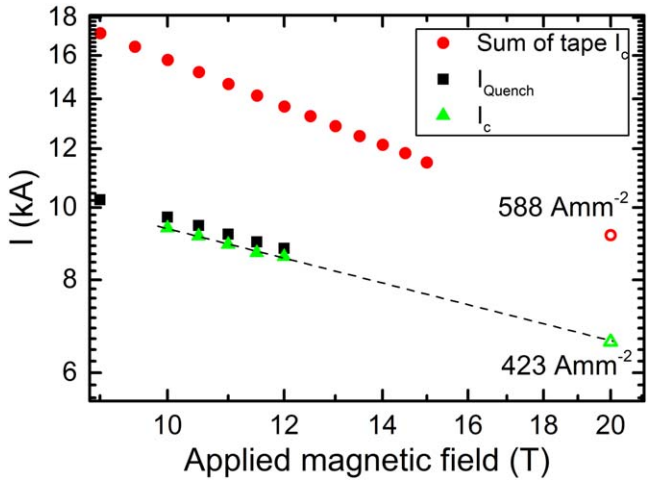

Figure 30. Magnetic field dependence of I_c and I_{quench} of the high-performance sample CORC®-W7, measured at 4.2 K. The dotted line is the fit to the I_c data using equation (4), with a value of $\alpha = 0.51$.

measurements performed at 4.2 K. The CORC® wire had an engineering current density of 598 A mm^{-2} at 10 T, which is 64% higher than reported for Roebel cables in perpendicular magnetic field [52, 53].

3.2.4. Future development of CORC® magnet wires. The initial production of REBCO tapes with 30 μm thick substrates in 2015 and their commercial availability from SuperPower Inc. since 2016 [29] has enabled the introduction of thin, highly flexible CORC® wires. Their performance with respect to engineering current density at 4.2 K at 20 T has recently exceeded that of CORC® cables, while carrying a current of at least 5–10 kA as required by many high-field magnets. A program awarded to Advanced Conductor Technologies and SuperPower Inc. by the Department of Energy, Office of High-Energy Physics, has as goal of introducing commercial REBCO tapes with even thinner substrates and CORC® wires wound from these tapes in 2019. First, tapes of 1, 1.5 and 2 mm width containing substrates of 25 μm thickness will become available at single piece lengths exceeding 100 m, followed by those containing substrates of 20 μm thickness.

Substrates of 25 μm and 20 μm thickness will allow for the introduction of the next generation of long-length, commercial CORC® wires containing formers of 2 and 1.6 mm thickness, respectively. The narrower tapes allow the CORC® wires to be wound from two tapes in parallel per layer, even when containing very thin formers, which is a key development to further improve the flexibility of the wire. At the same time, the relatively high tape count of between 30 and 50 in the CORC® wires ensures an operating current at 20 T in the range of 5–10 kA. Figure 31 shows the projected CORC® wire performance with respect to J_e and I_c at 20 T as a function of CORC® wire thickness when wound from tapes with 30, 25 and 20 μm thick substrates on formers of 2.4, 2 and 1.6 mm thickness, respectively. The performance is based on a tape I_c at 76 K of 35 A mm^{-1} width. The performance

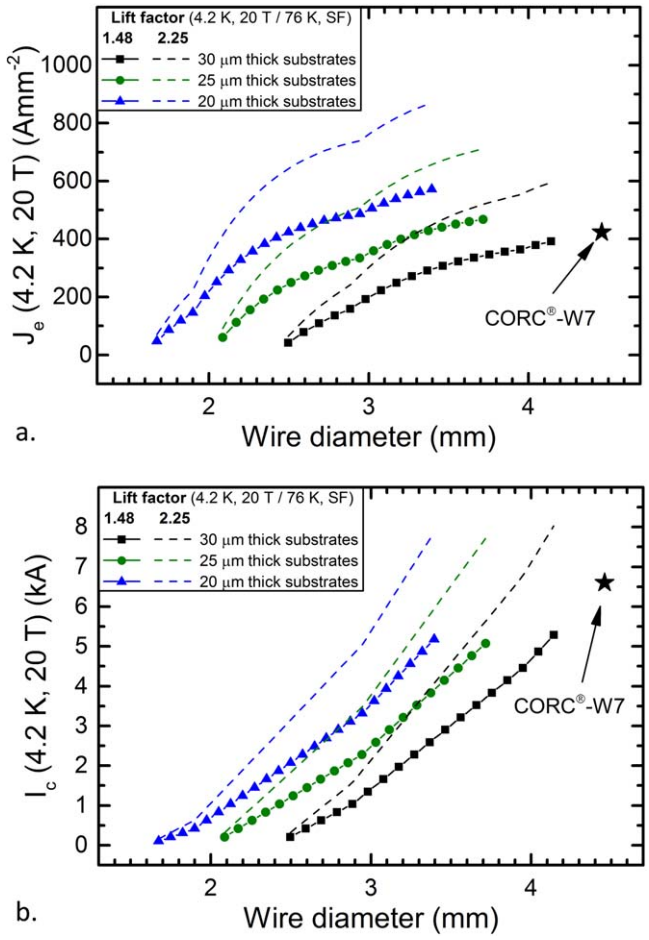

Figure 31. (a) Projected engineering current density, and (b) projected critical current as a function of CORC® wire thickness at 4.2 K in a background field of 20 T for CORC® wires containing substrates of 20, 25 and 30 μm thickness. The solid symbols indicate J_e based on a typical lift factor at 20 T of 1.48, while the dashed lines indicate J_e at a lift factor of 2.25.

projection for each CORC® wire configuration includes those using the typical lift factor of 1.48 at 4.2 K and 20 T (solid symbols) and the highest lift factor of 2.25 currently measured in production REBCO tapes. The current record J_e(20 T) of 423 A mm^{-2} in a 4.5 mm thick CORC® wire with lift factor 1.65 is included in the figure, although the sample had an I_c retention of 71.8%, while the performance projections are based on 100% I_c retention. Table 6 outlines some of the projected parameters of the CORC® wires containing tapes with 20 and 25 μm substrate thickness. Figure 31 and table 6 show that the next generation of CORC® wires allow J_e values at 20 T of between 500 and 800 A mm^{-2}. Such performance can be achieved in for instance a 3–3.5 mm thick CORC® wire containing tapes with 25 μm thick substrates and a lift factor of at least 2.25, or in a 2.5–3.5 mm thick CORC® wire containing tapes with 20 μm thick substrates and a lift factor of at least 1.48.

Conductor stability provided by the normal conducting material in the CORC® wire, often indicated by its copper fraction, is an important design parameter for high-field magnets. The CORC® wires outlined in tables 1 and 6 contain

Table 6. Projected performance of the next generation of CORC® wires.

		CORC® NGW1	CORC® NGW2	CORC® NGW3	CORC® NGW4	CORC® NGW5	CORC® NGW6
Type	—	Wire	Wire	Wire	Wire	Wire	Wire
Former size	(mm)	2	2	2	1.6	1.6	1.6
Tape number	—	16	31	49	16	31	50
Tape width	(mm)	2	2	2	2	2	2
Substrate thickness	(μm)	25	25	25	20	20	20
Number of layers	—	8	14	20	10	16	24
Outer diameter	(mm)	2.7	3.2	3.7	2.35	2.8	3.4
Cross-sectional area	(mm^2)	5.7	8.0	10.8	4.3	6.2	9.1
Hastelloy C-276 fraction[a]	—	0.21	0.29	0.34	0.22	0.30	0.33
Copper fraction[a]	—	0.63	0.51	0.43	0.57	0.48	0.39
I_c (76 K, s. f.)[b]	(A)	1120	2170	3430	1120	2170	3500
I_c (4.2 K, 20 T), LF = 1.48[c]	(A)	1658	3212	5076	1658	3212	5180
J_e (4.2 K, 20 T), LF = 1.48[c]	(A $mm^{2)}$	290	399	472	382	522	571
I_c (4.2 K, 20 T), LF = 2.25[c]	(A)	2520	4883	7718	2520	4883	7875
J_e (4.2 K, 20 T), LF = 2.25[c]	(A mm^{-2})	440	607	718	581	793	867

[a] With respect to total cross-sectional area.
[b] CORC® performance based on I_c of 35 A mm^{-1} tape width at 76 K and 100% I_c retention (no degradation due to cabling). s. f. = self-field.
[c] LF = lift factor defined as I_c(4.2 K,20 T)/I_c(76 K, s. f.). Listed I_c and J_e values are maximum calculated values at 100% I_c retention based on select single tape measurements up to 14.5 T, extrapolated to 20 T.

solid copper formers and have 5–20 μm thick copper plating on each tape. Their copper and Hastelloy C-276 fractions, calculated using the overall CORC® wire cross-section, are included in both tables. The copper fraction ranges from about 0.4 to about 0.7, which is close to the optimum fraction of 0.5 for high-performance magnet conductors. The Hastelloy C-276 fractions of around 0.2–0.4 provide the CORC® wire with significant mechanical strength during winding and operation that exceed the strength of most LTS and all other HTS conductors.

3.3. Performance of CORC® cables and wires under mechanical stress

Successful application of CORC® cables and wires in high-field magnets requires them to withstand the high stresses associated with high-field operation at high current. REBCO coated conductors generally have the highest mechanical strength with respect to irreversible tensile strain limit, in which the total strain range over which the change in I_c is fully reversible, is between 1.5% and 2% [14, 21]. REBCO coated conductors also can withstand the highest axial stress of any high-temperature superconductor. Both strengths are highly beneficial for CORC® cables and wires. The performance of CORC® cables and wires subjected to transverse compressive load and axial tensile stress is being investigated to determine their operating boundaries and to provide feedback that would allow these boundaries to reach even higher levels through further conductor optimization.

3.3.1. Effect of transverse compressive load on CORC® cables and wires.

Transverse compressive load is one of the predominant stresses that CORC® cables and wires will be subjected to when applied in large magnets that operate at very high currents, such as in fusion magnets. These magnets typically require bundling several CORC® cables or wires into a cable-in-conduit-conductor (CICC) to increase their operating current beyond that of a single cable (see section 5). The individual CORC® cables or wires within the CICC will not always benefit from the mechanical support provided by epoxy impregnation, as is typically the case in accelerator magnets. The CORC® cables or wires in the CICC may experience only limited support against the high transverse compressive loads that develop when the bundle carries a current of 50–100 kA in a 10–20 T background field. Understanding the effect of transverse compressive load on the performance of CORC® cables and wires is thus an important first step in the optimization of CORC® conductors for use in large magnet systems.

The method used to apply transverse compressive load to CORC® cables and wires in liquid nitrogen is shown in figure 32. The CORC® cable or wire is placed between two flat stainless steel anvils, resulting in a line contact between them. The bottom anvil is part of the load reaction frame attached to the servo-hydraulic actuator, while the 50 mm long top anvil is attached to the piston. Figure 33 shows a CORC® wire placed on the 115 mm long bottom anvil, while the entire bottom part of the load frame is located in an

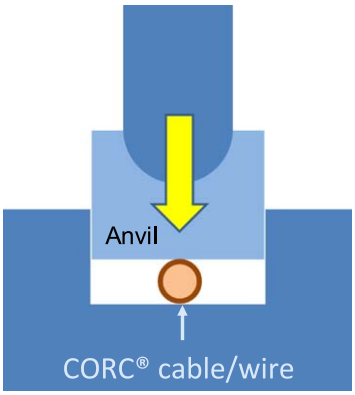

Figure 32. Overview of a CORC® wire located between two flat stainless steel anvils. Reproduced from [54]. © IOP Publishing Ltd. All rights reserved.

insulating foam container that will be filled with liquid nitrogen. The CORC® wire is attached to two copper adapters that allow currents in excess of 2000 A to be injected into the CORC® wire.

The dependence of I_c on transverse compressive load and the *E–I* characteristics measured at different loads at 76 K are shown in figure 34 for sample CORC®-W4 (table 1), which was a CORC® wire with 2.55 mm thick former. Because the actual width of the contact area between the two anvils and the CORC® wire was unknown and likely changed with load, the applied load in kN m^{-1} is reported instead of the applied stress in MPa. The CORC® wire I_c remained unchanged until a load of about 115 kN m^{-1} was applied. Further increase in transverse load resulted in a gradual shift of the *E–I* curves and I_c to lower currents. The transverse load of 115 kN m^{-1} would be reached in a CORC® cable or wire, which is located in the jacket of a CICC that isolates the conductor from potential interaction from neighboring magnet windings, that would operate at a current of 5.75 kA in a background field of 20 T.

The performance of several CORC® wires (CORC®-W2 and CORC®-W4) and a CORC® cable (CORC®-C4), each having a different former size, tape width and tape count, were measured as a function of monotonic transverse loading at 76 K. The gap spacing in the three samples was comparable at about 0.3–0.4 mm, removing gap spacing as a parameter in the comparison. A more detailed investigation in the effect of gap spacing will be provided elsewhere [54]. Figure 35 compares the normalized I_c as a function of applied load of three samples with different layouts. CORC® wires containing 2.55 mm thick formers (CORC®-W4), resulting in a maximum winding strain of the inner tapes of −1.16%, started degrading at the lowest load, followed by the CORC® cable with 4.9 mm thick former and −1.00% maximum winding strain (CORC®-C4) and by the CORC® wire with 3.2 mm thick former and −0.93% maximum winding strain (CORC®-W2). The critical load of sample CORC®-W2 was 217 kN mm^{-1}, which would be reached at an operating current of 10.8 kA in a 20 T background field. Table 7 shows the critical transverse loads for the three different samples, defined at different percentages of I_c reduction. The difference in critical load between the three samples correlates with the maximum REBCO film strain of

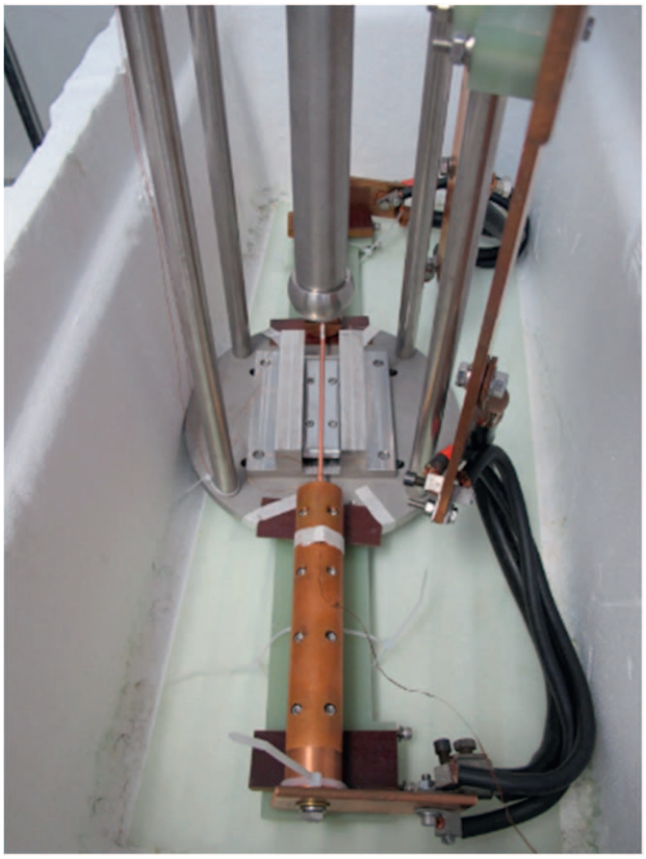

Figure 33. A CORC® wire being installed into the load frame, before the top anvil is placed onto the sample. Reproduced from [54]. © IOP Publishing Ltd. All rights reserved.

the tapes in the inner layer. Any deformation of the former under transverse load would likely bring the winding strain closer to the irreversible strain limit under axial compression of about −1.25%, and once exceeded, would cause I_c of the inner tapes to decrease sharply.

Increasing the thickness of the former, in combination of a reduction of the substrate thickness of the tapes, will result in a lower strain state of the REBCO film in the inner tape layers of the CORC® cable or wire. A reduction in strain state and the use of formers with a higher yield stress, such as work hardened copper or copper alloys, will likely increase the irreversible load limit of CORC® cables and wires under transverse compression.

A major advantage of CORC® cables and wires when applied to magnets in which they experience high transverse compressive stresses over other HTS cables is that CORC® conductors can be optimized to withstand high transverse loads without the need for epoxy impregnation or external reinforcement. Roebel cables, on the other hand, require epoxy impregnation to provide them with sufficient strength to survive transverse stresses during operation [55, 56]. The resilience of TSTC against transverse compressive stress is potentially even more problematic. Significant degradation in I_c was measured as soon as the transverse compression is applied to the twisted tape stack at an angle other than perpendicular to the tape plane [57]. Significant external

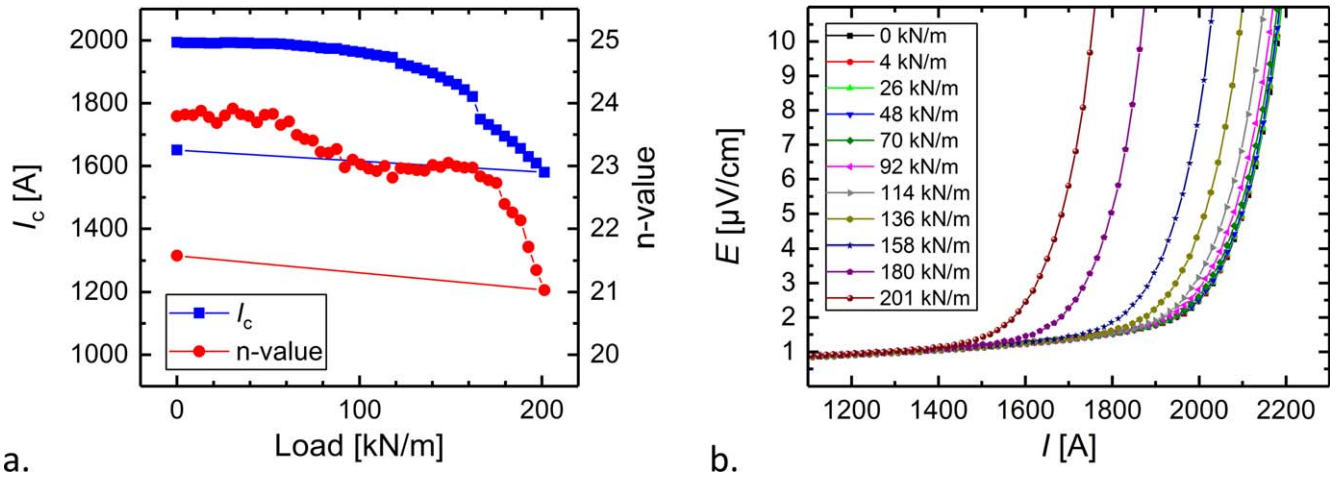

Figure 34. (a) Dependence of I_c and n-value on transverse compressive load at 76 K of sample CORC®-W4 containing 27 tapes of 2 mm width. (b) E–I curves measured at different transverse loads.

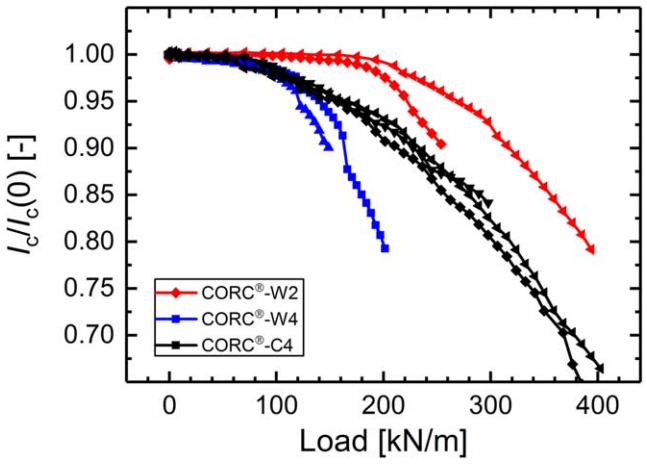

Figure 35. Normalized I_c as a function of applied transverse load at 76 K, measured on several CORC® wires and cables. All samples were wound with 0.3–0.4 mm gap spacing between their tapes.

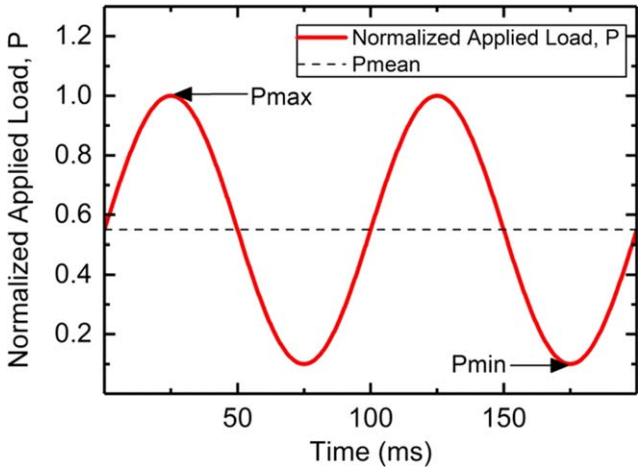

Figure 36. Waveform outlining the transverse compressive load cycle with $P_{min}/P_{max} = 0.1$.

Table 7. Critical transverse load in kN m^{-1} at 76 K for different CORC® cables and wires.

I_c/I_{c0}	CORC®-W2	CORC®-W4	CORC®-C4
0.97	217	115	124
0.95	243	133	160
0.9	284	163	226

reinforcement of TSTC would thus be required to make them more resilient against transverse compressive stress, although the majority of the transverse load originates from within the stack due to the electromagnetic nature of transverse load.

The effect of transverse compressive load cycling, up to 100 000 cycles, on the critical current of CORC® cables has also been determined. The load was cycled at 76 K in a sinusoidal function between 10% (P_{min}) and 100% of the peak load (P_{max}) (see figure 36). Figure 37 shows an example where the I_c for sample CORC®-C4 remained unchanged following 100 000 cycles at a peak load of 210 kN/m where

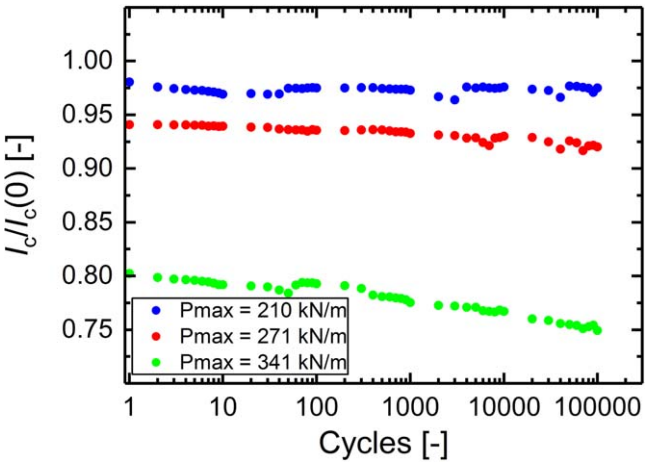

Figure 37. Dependence of the normalized I_c on stress cycling at 76 K of sample CORC®-C4 wound with 0.1 mm gap spacing between tapes at 210 kN m^{-1}, corresponding to 97.5% I_c retention, 271 kN m^{-1}, corresponding to 94% I_c retention, and 341 kN m^{-1}, corresponding to 80% I_c retention.

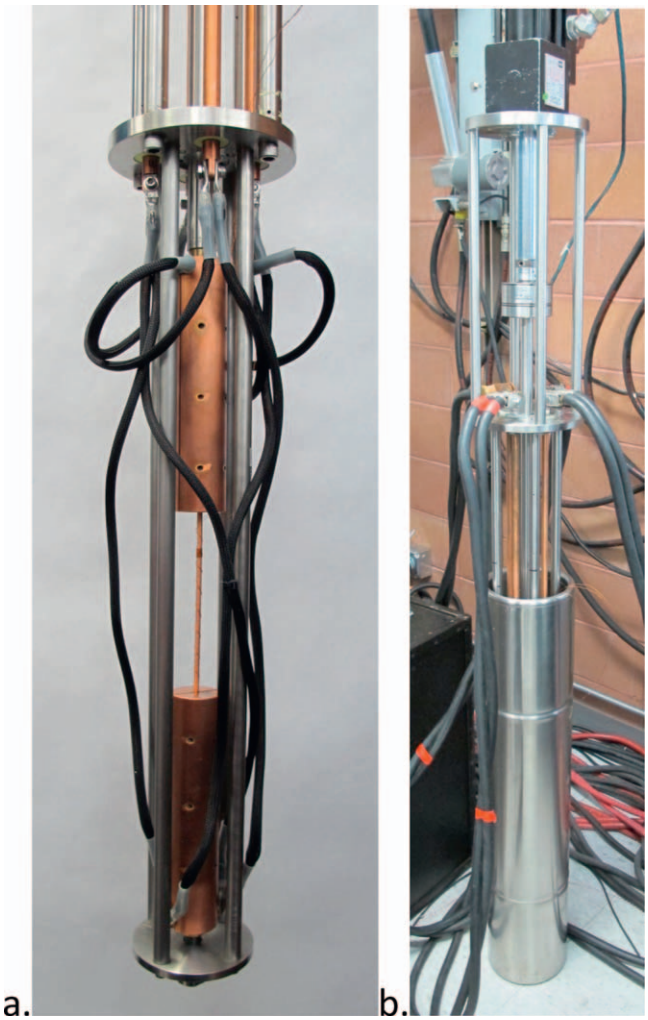

Figure 38. (a) A CORC® wire mounted with the copper adapters in the axial tension device. (b) The sample being loaded in the open liquid nitrogen cryostat. Reproduced from [58]. © IOP Publishing Ltd. All rights reserved.

I_c initially degraded by 3%. This particular sample was wound with only 0.1 mm gap spacing between tapes, compared to 0.3–0.4 mm for sample C4 shown in figure 35. Only once higher peak loads were applied and the initial I_c decreased significantly, did I_c decrease further with cyclic loading: starting at 94%, I_c dropped to 92%, and starting at 80%, I_c dropped to 75%, both after 100 000 cycles applied in liquid nitrogen. These results are very promising for CORC® cables when applied in CICC, because they indicate that when the CORC® cable would be operated below, or even slightly above its irreversible transverse load limit, I_c is not expected to degrade significantly even after 100 000 load cycles. Further results, including cyclic load performed on CORC® wires have been published elsewhere [54].

3.3.2. Effect of axial tensile stress on CORC® wires. Another important stress to consider for application of CORC® cables and wires in high-field magnets is axial tensile stress. Knowledge of the axial stress limit is an important magnet design parameter, and further conductor optimization could be considered to increase this limit.

Stress is applied to CORC® wires using a servo-hydraulic actuator and two copper adapters that clamp directly onto the wire terminals (figure 38). The sample is lowered into an open cryostat filled with liquid nitrogen that allows measuring the critical current exceeding 2000 A at axial tensile loads of up to 13.3 kN.

Figure 39 shows I_c as a function of axial tensile stress at 76 K for three samples of layout CORC®-W9, which were CORC® wires containing a 2.55 mm thick copper former and 30 tapes of 2 mm width. The figure also includes select *E–I* curves of one of the samples measured at different stresses. The terminals were filled with 63Sn–37Pb solder, instead of 100In solder, because the axial stress was transferred from the terminals to the CORC® wire and indium solder was unable to transfer the load due to its very low yield strength.

The critical current of the CORC® wires remained unchanged until a critical stress of about 170 MPa was reached, after which a rapid decrease in I_c with stress was measured. No reversible change in I_c, which is present in single coated conductors under axial tension (figure 1), was measured until the critical stress was reached. The absence of a reversible strain effect in CORC® wires can be explained by the winding angle of between 35° and 47° at which the tapes are wound into the CORC® wires. At this angle, the reversible strain effect almost disappears completely [20]. The winding angle also results in the stress applied along the CORC® wire axis to be at an angle close to 45° with respect of the tape axis, with the consequence that the applied axial stress has no significant effect on T_c and thus I_c. A more detailed overview of the behavior of CORC® wires under axial stress, including stress cycling, will be reported elsewhere [58].

The irreversible tensile stress limit is most likely determined by the constituents of the CORC® wire, such as the number of tapes, the yield stress of the tapes, the thickness of the former and the yield stress of the former. The critical current of the CORC® wire is expected to degrade irreversibly as soon as the substrate of the tapes yield. The CORC® wires of this study contained solid, annealed copper formers, which have a relatively low yield stress [58]. Increasing the yield strength of the former, by for instance using a harder grade of copper, will likely result in a further improvement of the irreversible tensile stress limit of the CORC® wire.

4. CORC® power cables and wires

4.1. Helium gas cooled CORC® power cables

One of the programs to develop CORC® cables for power applications was awarded to Advanced Conductor Technologies by the US Navy with the goal to develop and demonstrate a 10 m long, two-pole CORC® dc power cable. Instead of operating the power cable in liquid nitrogen, such as was done with earlier HTS power cables [1–3], the Navy required the coolant to be pressurized helium gas to reduce asphyxiation hazards associated with the use of liquid cryogens in

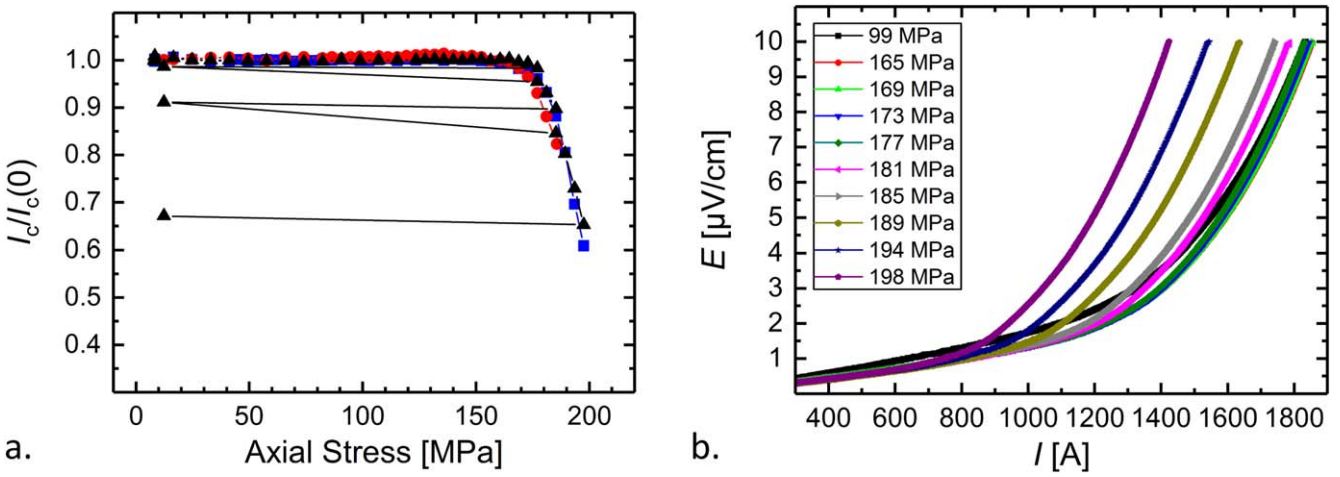

Figure 39. (a) Normalized I_c of three samples CORC®-W9 measured at 76 K as a function of axial tensile stress, including I_c values after unloading the stress. (b) *E–I* characteristics measured at different axial stress levels.

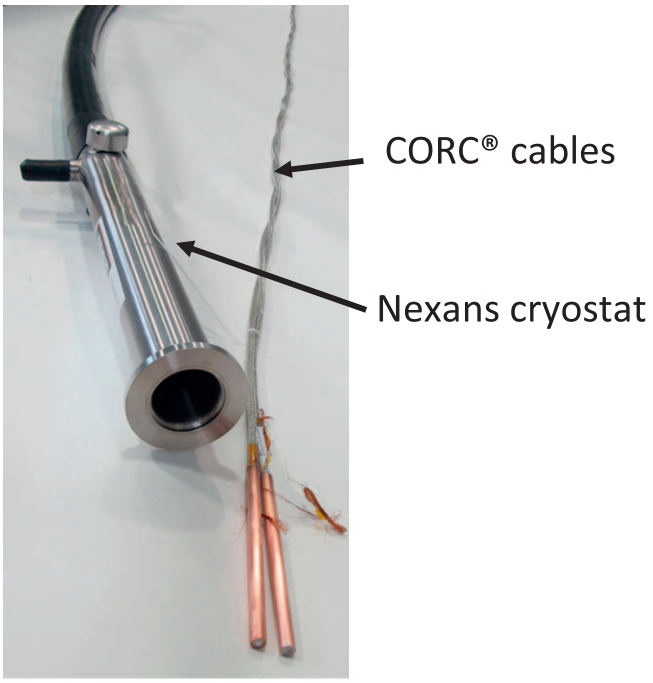

Figure 40. Overview of the 10 m long CORC® dc power cable consisting of two twisted CORC® cables (CORC®-C1) and the flexible cryostat through which it would be pulled. Reproduced from [17]. © IOP Publishing Ltd. All rights reserved.

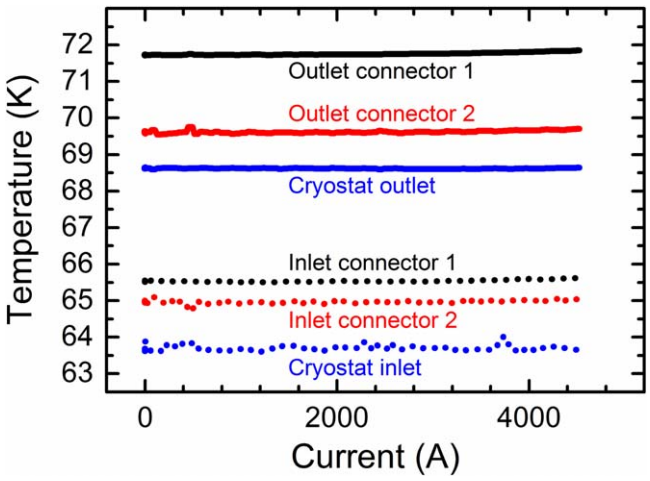

Figure 41. Temperature as a function of current during the two-pole operation of cable CORC®-C1 in helium gas. Reproduced from [17]. © IOP Publishing Ltd. All rights reserved.

confined spaces. One of the benefits of cooling with gaseous helium is that the operating temperature can be significantly lower than is possible with liquid nitrogen, taking advantage of the significant increase in I_c of REBCO with a reduction in temperature. One of the challenges with using helium gas as a coolant is its relatively low cooling power and thus the requirement to operate at gas pressures of up to 20 bars to ensure sufficient mass flow of between 5 and 10 g s^{-1}.

The two-pole CORC® power cable was developed by twisting two monopole CORC® cables together (CORC®-C1 in table 1) and pulling the cable through a 10 m long Nexans cryostat [17] (figure 40). Several layers of polyester heat shrink tubing was applied to provide insulation to the cable, although the cable was not tested at voltages exceeding 10 V. Superconducting CORC® feeder cables were also developed to inject current into the power cable located in the helium gas cryostat. Low-resistant connections between the terminations of the power and feeder cables ensured a minimal dissipation through Ohmic heating within the helium gas environment, while liquid nitrogen was used to cool the copper current leads coming from room temperature.

The two-pole CORC® power cable and the CORC® feeder cables were designed for an operating current of 4 kA/pole at 50 K that would require their I_c to be at least 6 kA at that temperature. The cable was tested in pressurized helium gas at a temperature between 63 K at the helium gas inlet and 72 K at the helium gas outlet (figure 41). The temperature rise along the length of the power cable was caused mainly by the thermal conduction through the cryostat flanges that separated the helium gas and liquid nitrogen environments of the custom cryostats holding the CORC® feeder cables. The temperature of the different components in the power cable system

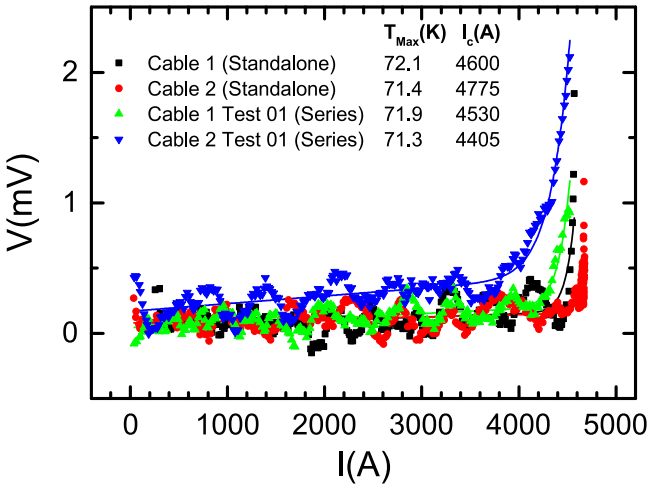

Figure 42. *V–I* curves of the two poles of cable CORC®-C1 in helium gas at a maximum temperature of about 72 K measured on the connector at the outlet side of the cryostat. The poles were energized separately and when connected in series. Reproduced from [17]. © IOP Publishing Ltd. All rights reserved.

did not increase with current up to the maximum current of about 4700 A.

Both poles of the CORC® power cable were tested individually up to a current of about 4.5–4.7 kA where the superconducting transition occurred (figure 42). No transition from the superconducting to the normal state of the four CORC® feeder cables was measured, as they were designed with a significant current margin compared to the power cables. Both poles of the CORC® power cable were connected in series, thereby having each pole experience the magnetic field generated by the neighboring pole. The critical current of each pole was reduced by less than 10% due to the higher magnetic field on both cables.

The cable could not be tested at 50 K due to the heat load through the cryostat flanges and the limited cooling power of the Stirling helium gas circulation system. The superconducting transition in the CORC® power cable is expected to occur at the location experiencing the highest temperature, which was the cable termination near the helium gas outlet. The highest temperature of about 72.5 K and the temperature dependence of I_c suggests that the CORC® power cable would have an I_c of between 12 and 14 kA at 50 K, allowing for an operating current of between 8 and 9 kA per pole.

4.2. CORC® FCL wires

Another potential important application of CORC® cables, and especially CORC® wires, is their use as FCL conductors in dc power systems that would protect equipment from over-currents [3, 59, 60]. The rapid transition of HTS from the superconducting state into the normal state when the current exceeds I_c results in a significant voltage generation over the CORC® wire length, rapidly increasing its impedance that in return limits the over-current. CORC® wires are able to generate large voltages without burnout likely due to their relatively short tape twist pitch and thus potential for significant current sharing

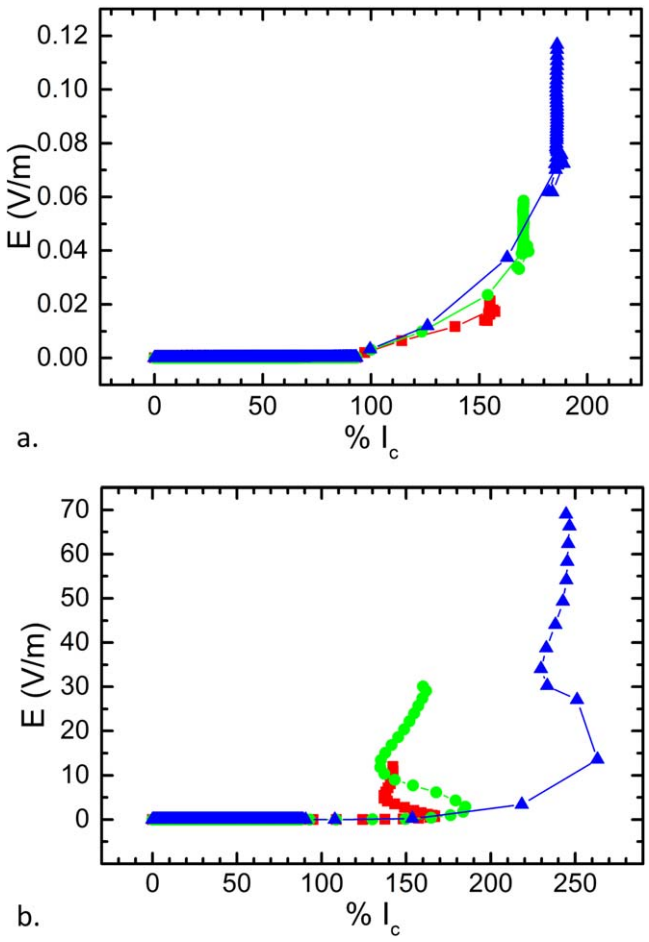

Figure 43. Electric field as a function of various applied overcurrents at 76 K for (a) a CORC® FCL wire containing a solid copper former (CORC®-W3), and (b) a CORC® wire containing a solid stainless steel former (CORC®-W8). The time between data points is 1 ms. Reproduced from [61]. © IOP Publishing Ltd. All rights reserved.

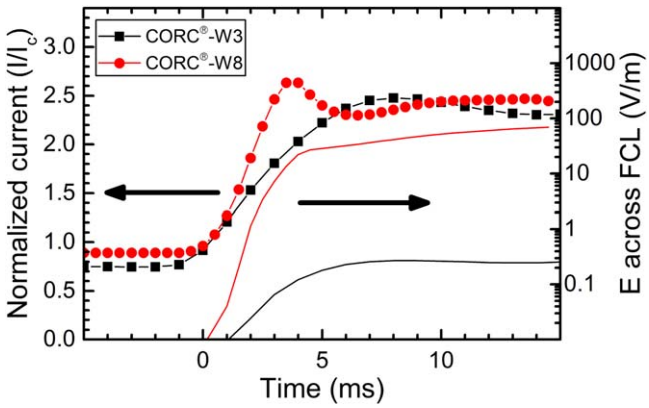

Figure 44. Applied overcurrent (I/I_c) as a function of time (symbols) and corresponding electric field (lines) for two CORC® FCL wires tested up to about 250% of I_c at 76 K. Reproduced from [61]. © IOP Publishing Ltd. All rights reserved.

between tapes, making them the ideal building block for any high-current FCL device or cable [61].

Figure 43 shows the voltage response as a function of CORC® wire current, expressed in percentage of I_c, of two

CORC® wires in liquid nitrogen at 76 K (CORC®-W3 and CORC®-W8). The current is pulsed from 90% of I_c to a maximum current value exceeding I_c, ranging from 150% to 250% of I_c. This causes a rapid heating of the CORC® wire and subsequent increase in voltage over time. The main difference between the two samples is their former, being either solid copper (CORC®-W3 in figure 43(a) with I_c of 646 A) or solid stainless steel (CORC®-W8 in figure 43(b) with I_c of 1124 A), besides the number of tapes (16 in CORC®-W3, and 18 in CORC®-W8). The much higher electrical resistivity of the stainless steel former resulted in a much more rapid voltage increase at a given overcurrent pulse, compared to the sample with copper former. Note the ringing of the power supplies when the current is increased rapidly, as seen in figure 43(b).

The response of both CORC® FCL wires as a function of time (figure 44) clearly shows the effect of the resistivity of the former on the response the CORC® wire to overcurrent. Sample CORC®-W3 containing a solid copper former developed an electric field over its length of about 0.2–0.3 V m^{-1} within 5 ms after a current of 2.5 times I_c was applied, while sample CORC®-W8 developed an electric field of 20 V m^{-1} under the same conditions. The electric field of sample CORC®-W8 increased to about 70 V m^{-1} after 20 ms before the current was switched off. As explained in more detail in [61], CORC® FCL wires are capable of ms response time that allows sufficient time for mechanical switchgear that requires at least 15 ms to disconnect the superconducting cable. The rapid increase in temperature of the CORC® wires during each overcurrent event, followed by immediate quenching to 76 K, did not have any influence on the conductor performance, even after more than 100 fault cycles [61]. The versatile layout of CORC® wires, the effective current sharing between their tapes, and their robustness against over currents and rapid temperature changes make them highly effective FCL conductors.

5. CORC® cables for fusion and detector magnets

Large magnets for fusion machines and particle detectors often require very high operating currents in excess of 50 kA that cannot be achieved in a single LTS or HTS cable. Several superconducting cables, or strands, need to be bundled and placed into a metal jacket to form a high-current CICC that is cooled with liquid or forced-flow supercritical helium, or potentially with helium gas. Several approaches to develop high-current CORC®-CICC for large magnet systems are outlined in the following sections.

5.1. CORC® cables configured into a 6-around-1 CORC®-CICC

High-current CORC®-CICC for use in fusion and detector magnets, with the goal of reaching a current of 80 kA at 4.2 K in a background field of 10.9 T, are being developed as part of a collaborative effort between CERN in Switzerland, the University of Twente in the Netherlands and Advanced Conductor Technologies [62–64]. The approach is centered on bundling six CORC® cables around a central cooling tube, forming a 6-around-1 configuration. The bundle is placed within a rectangular stainless steel jacket to form a

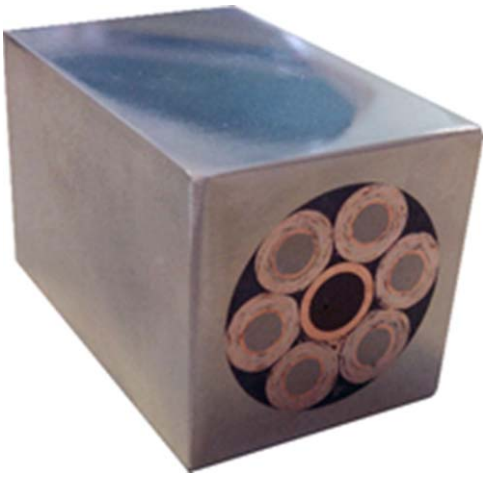

Figure 45. Cross-section of a 6-around-1 CORC®-CICC based on CORC® cables. © 2016 IEEE. Reprinted, with permission, from [62].

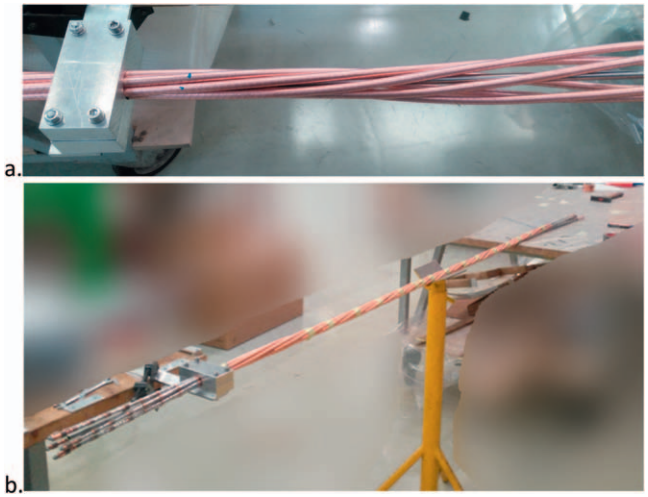

Figure 46. (a) Six CORC® cables being wound around a stainless steel tube. (b) Completed bundle of CORC® cables to form a 6-around-1 CORC®-CICC. Reproduced with permission from [64].

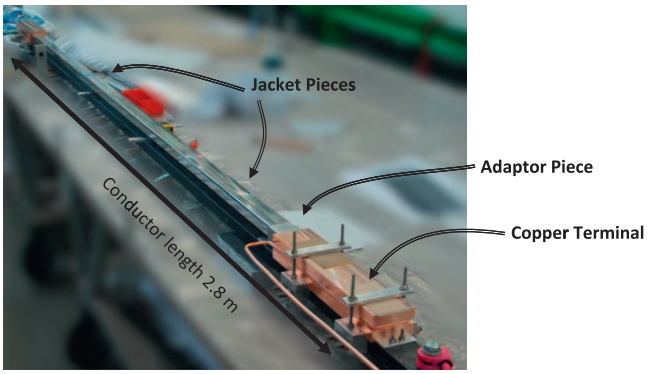

Figure 47. Overview of the fusion CORC®-CICC sample. Reproduced with permission from [64].

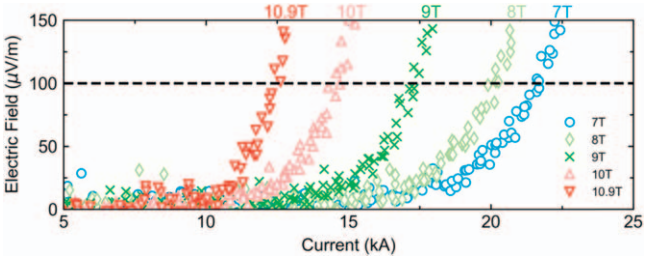

Figure 48. Electric field versus current of the fusion CORC®-CICC containing a stainless steel jacket measured in SULTAN at 50 K in fields between 7 T and 10.9 T. The dotted line is the criterion at which I_c is defined. Reproduced with permission from [64].

CORC®-CICC for fusion magnets (figure 45), or a copper jacket for detector magnets. Coolant flows within the jacket for the fusion conductor, while the detector conductor also allows cooling from the outside of the jacket through conduction.

Two 3 m long CORC®-CICC samples were prepared for testing in the SULTAN test facility at the Paul Scherrer Institute in Switzerland, consisting of a 10.9 T split-pair solenoid magnet, into which both straight samples were inserted while being connected in series. Both samples contained 6 CORC® cables (CORC®-C3 in table 1) wound around a stainless steel cooling tube at a twist pitch of about 0.4 m (figure 46). One of the samples contained a stainless steel jacket (figure 47), while the other sample contained a copper jacket.

Initial tests of both CORC®-CICC samples were performed in SULTAN [64], in which the critical current of the samples was measured as a function of magnetic field and temperature. The samples were cooled with liquid helium for measurements performed at 4.2 K, and with helium gas for measurements up to 60 K. Mechanical degradation to the CORC® cables in the detector magnet CORC®-CICC containing the copper jacket limited the tests to currents below 50 kA for both samples that were connected in series. Later examination determined a level of degradation of about 50% of all six CORC® strands in the bundle of the detector sample. The *E–I* curves of the fusion CORC®-CICC with stainless steel jacket that did not degrade were measured at 50 K in magnetic fields between 7 T and 10.9 T, and are shown in figure 48. The resistive voltage measured over the terminations was subtracted from the data. The critical current of the CORC®-CICC was also measured between 45 and 50 K for magnetic fields as low as 7 T (figure 49). The test was limited to a highest current of about 30 kA due to the degraded sample with copper jacket. This current was reached at 45 K in a 7.5 T background field. The degraded sample is currently being replaced and further testing up to 80 kA at 4.2 K in 10.9 T is expected at the end of 2018, or beginning of 2019.

5.2. CORC®-CICC development for use in compact fusion magnets

The rapid development of REBCO coated conductors and various approaches to bundle them into high-current cables opens the door for high-field, compact fusion magnets that have the potential to significantly speed up the development

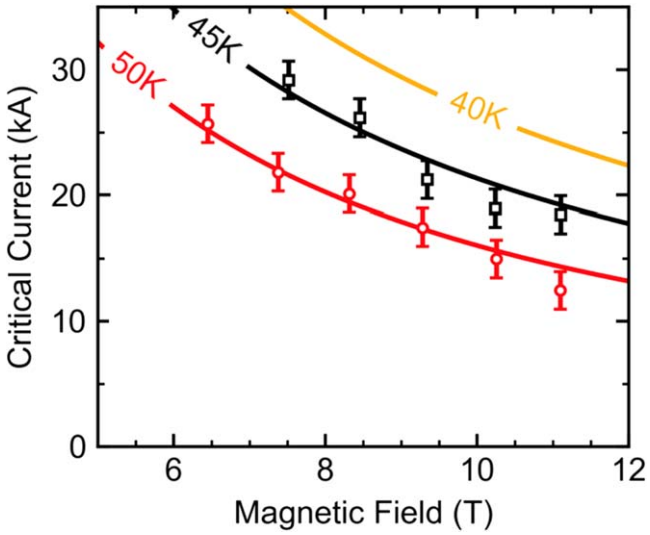

Figure 49. Magnetic field dependence of I_c of the fusion CORC®-CICC measured at different temperatures. The solid lines are the expected I_c values. Reproduced with permission from [64].

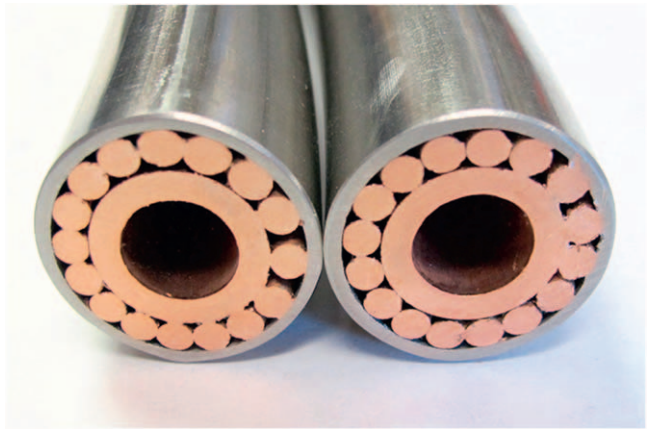

Figure 50. Cross-section of a model CORC®-CICC containing copper strands of 3.85 mm in diameter after bending of the CICC to 1 m diameter.

of fusion as a viable energy source [65]. Several approaches to develop compact fusion magnets are underway in which initial magnet systems were demonstrated using copper coils [66], or even with REBCO tapes [67]. Most compact fusion magnet designs require high-current windings and thus REBCO cables, with winding diameters of no more than several meters.

CICC based on CORC® cables, such as the 6-around-1 design outlined in the previous section, likely will not allow for bending to diameters required by most compact fusion magnet concepts. The flexibility of the CORC®-CICC depends in part on the twist pitch length at which the CORC® strands are bundled, but also on the thickness of the CORC® strands and their ability to slide within the bundle during bending of the CICC. Advanced Conductor Technologies is developing highly flexible CORC®-CICCs, based on CORC® wires, for use in compact fusion magnets. The CICCs contain between 10 and 20 CORC® wires wound with a short twist

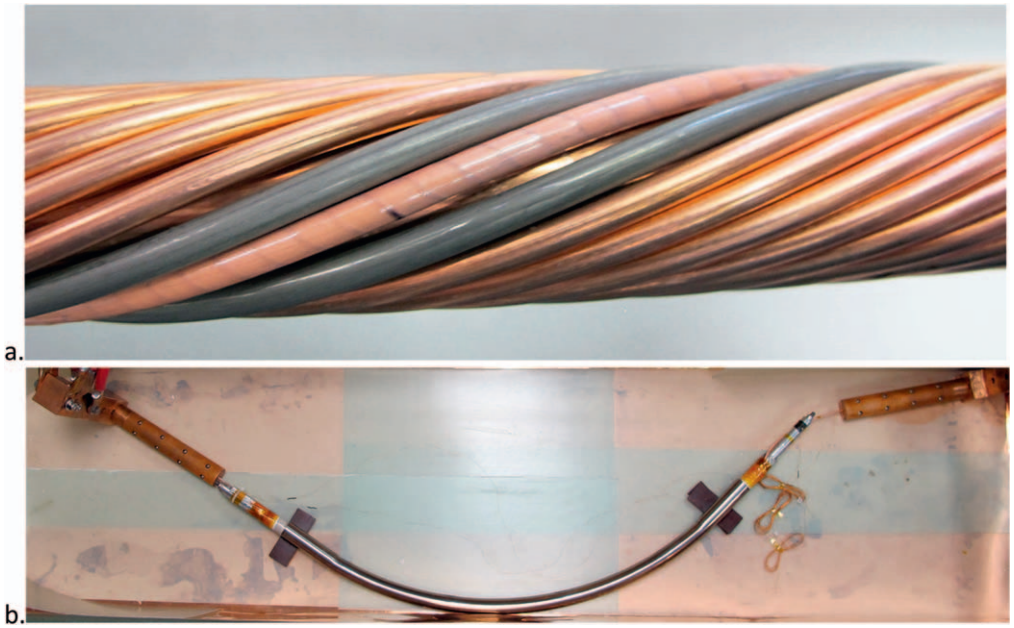

Figure 51. (a) Model CORC®-CICC containing 13 copper strands and one CORC® wire containing a layer of polyester insulation, surrounded by two stainless steel strands. (b) The CORC®-CICC bent to 1 m diameter, ready for testing in liquid nitrogen.

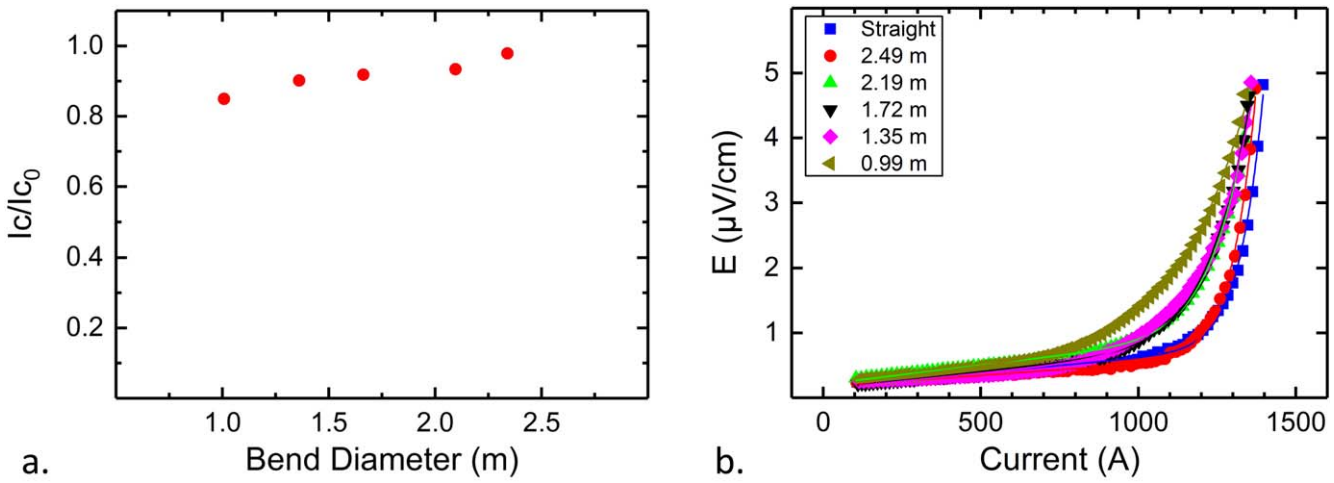

Figure 52. (a) Normalized I_c measured at 76 K as a function of bending diameter of the CORC®-CICC containing copper strands, one 3.65 mm thick CORC® wire and two stainless steel strands of 4.1 mm in diameter surrounding the CORC® wire. (b) *E–I* curves of the CORC®-CICC measured at 76 K at different bending diameters of the CICC.

pitch in the order of 100–300 mm around a larger cooling tube, as demonstrated with copper strands in figure 50. The large number of CORC® strands in combination with the relatively short twist pitch results in a relatively flexible CICC, but also a much higher level of transposition between the strands compared to CICCs based on thicker CORC® cables. A higher degree of transposition reduces the ramping losses and results in a more even current distribution between the strands at high current ramp rates. The high performance of CORC® wires would potentially allow the CORC®-CICC to carry currents between 50 and 100 kA at 20 T.

Initial verification of the flexibility of CORC®-CICC based on CORC® wires has been performed on a model CORC®-CICC containing 13 copper strands of 3.85 mm in diameter and one CORC® wire (CORC®-W2 in table 1) that was surrounded by two stainless steel strands of slightly larger diameter (4.1 mm compared to 3.85 mm for the copper strands and CORC® wire) (figure 51(a)). The slightly thicker stainless steel strands prevent the stainless steel jacket from compressing the CORC® wire during bending. The model CORC®-CICC was bent at room temperature to diameters ranging from 2.3 m down to 1 m (figure 51(b)) and I_c of the CORC® wire was measured in liquid nitrogen for each bending diameter. Figure 52 shows the normalized I_c of the CORC® wire degrading only slightly during bending, where it remained at 82% of its initial value after the CORC®-CICC was bent to a diameter of 1 m.

Further optimization of CORC®-CICC based on either CORC® cables or wires, involves mechanically decoupling each CORC® strand from its neighbors, which would enable

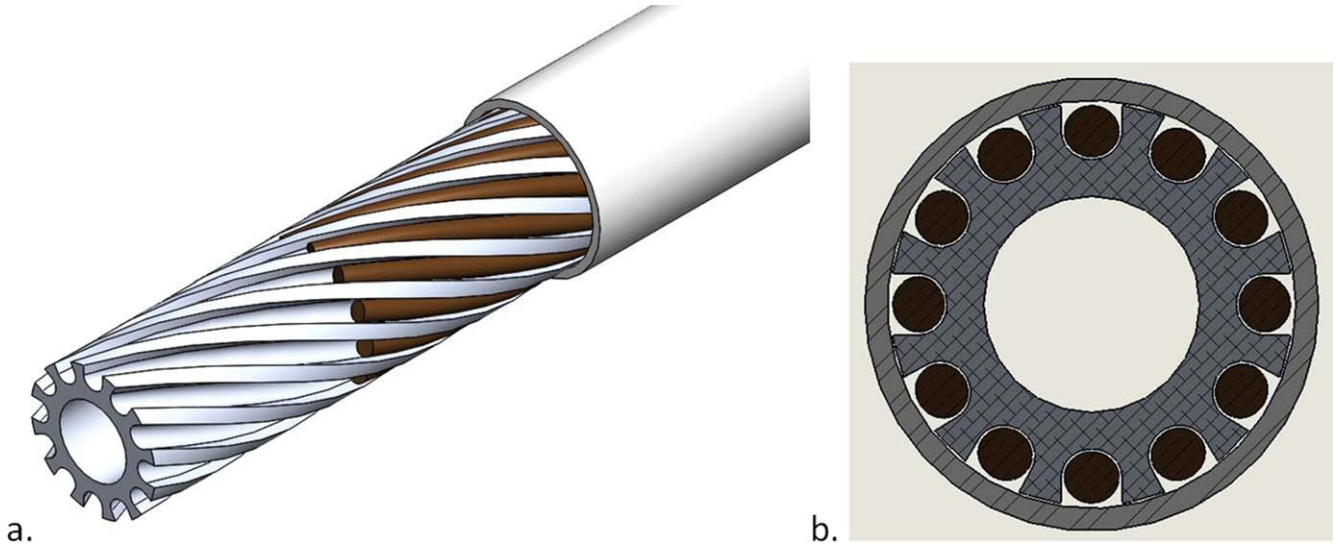

Figure 53. (a) Example of a CORC®-CICC with extruded structure in which the CORC® wires are placed. The fins between the CORC® wires extend to the outer jacket, and allow the CORC® wires to slide during CORC®-CICC bending. (b) Cross-section of the CORC®-CICC which shows the CORC® wires located within the grooves.

easier bending by allowing the CORC® strands to slide freely. Decoupling would also significantly reduce the transverse compressive stresses on each strand during operation. One of the reasons why one of the 6-around-1 CORC®-CICC samples degraded during the earlier SULTAN test (section 5.1) was the accumulative transverse compressive stress on the CORC® cables during high-current operation at high magnetic field. The CORC® cables were designed to withstand these accumulative stresses, but slight variations in cable manufacturing parameters and the CICC jacket having incorrect tolerances may have resulted in movement of the cables in the bundle during operation. Such movement could prevent the individual cables from correctly reacting the transverse forces, causing irreversible degradation [64].

One approach to mechanically decouple the CORC® strands in the bundle, which follows the design introduced by ENEA [34], is to place them within an extruded structure that forms the central tube, but also contains fins that contact the jacket, while the CORC® strands are positioned in the channels between the fins. Figure 53 shows an example of a CORC®-CICC containing an extruded central aluminum or copper structure in which 12 CORC® wires are positioned.

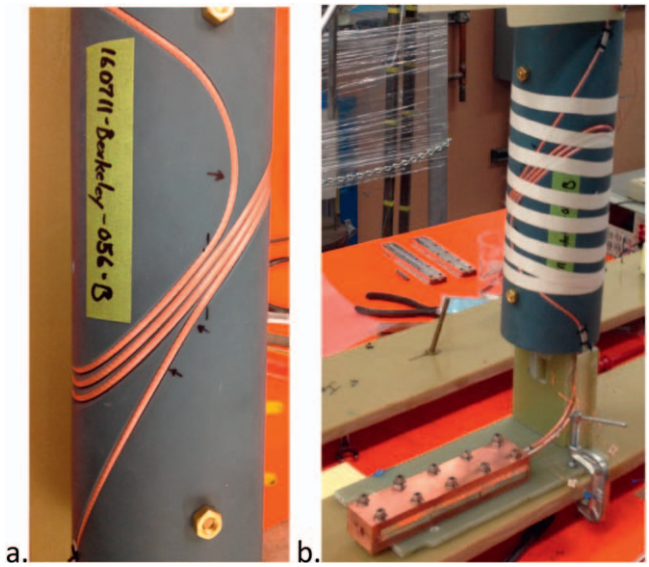

Figure 54. (a) Outermost layer of the three-turn CCT structure in which wire CORC®-W3 was wound. (b) Assembled two-layer CCT structure and 'praying hands' joint at bottom connecting the inner layer to the outer layer. Reproduced from [16]. © IOP Publishing Ltd. All rights reserved.

6. CORC® wire development for high-field accelerator magnets

The introduction of CORC® wires in 2016 [14] that allow bending to much smaller diameters than CORC® cables, while having relatively high I_c and J_e values at high magnetic fields, enables a more rapid development of the next generation of high-field particle accelerator magnets. One of the efforts to develop low-inductance accelerator magnets from CORC® wires currently underway is a collaboration between Lawrence Berkeley National Laboratory (LBNL) and Advanced Conductor Technologies. CORC® wires are being wound into canted cosine-theta (CCT) magnets [16], which is a conductor-friendly design in which the conductor windings are mechanically supported by placing them into a groove machined within the magnet mandrel [68].

The near-term goal of the program is to demonstrate a 5 T standalone CCT magnet with 50 mm aperture wound from CORC® wires, followed by a long-term goal to develop a high-field insert CCT magnet that would increase the field of a 12–15 T LTS CCT outsert magnet to 20 T. The near-term goal of generating 5 T will be approached in three steps. The first step is to wind a two-layer, 40-turn per layer CCT coil (CCT-C1) that should reach 1 T using about 50 m of low-J_e CORC® wire (CORC®-W3 in table 1). Initial tests on three-

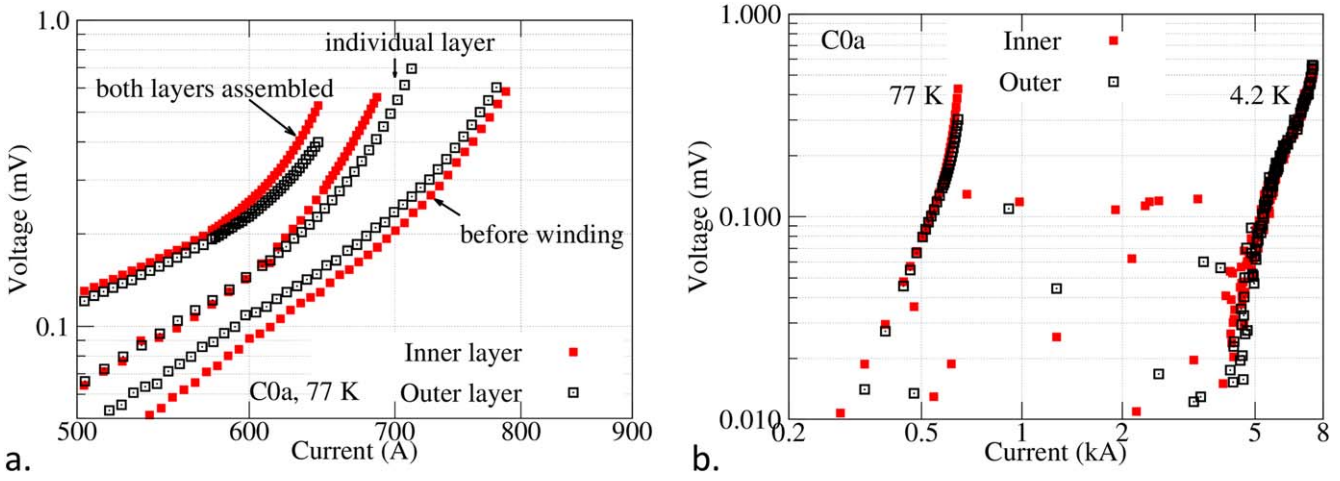

Figure 55. (a) Voltage measured across the magnet layers as a function of current for the first three-turn CORC® CCT dipole at 77 K and at 4.2 K, in self-field. (b) Layer voltage as a function of current for the three-turn CCT dipole at 77 K and 4.2 K in self-field. Reproduced from [16]. © IOP Publishing Ltd. All rights reserved.

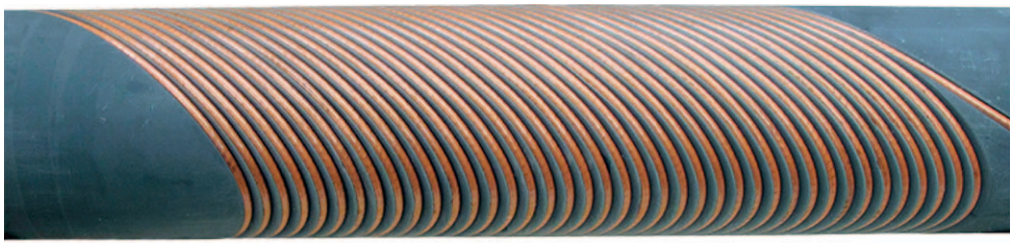

Figure 56. The outer layer of the two-layer CCT magnet CCT-C1 containing about 15 m of CORC® wire (CORC®-W3).

turn mandrels (figure 54) that demonstrated that the CORC® wire could withstand the required minimum bending radius of 25 mm at the poles were successfully completed [16]. Figure 55(a) shows the *V*–*I* characteristics of the CORC® wires measured at 77 K before and after winding onto the CCT mandrels. The critical current decreased from about 750 A to about 680 A after winding, and to about 650 A when both layers were combined. The decrease in I_c was largely due to the increased magnetic field on the wire. The two-layer, three-turn per layer CCT magnet was also tested at 4.2 K, where the CORC® wires had an I_c of about 6 kA with a peak field on the conductor of about 1.2 T at the highest current of 7.5 kA. At that current, the dipole field was about 0.5 T.

After the successful test of the three-turn CCT structures, two 25 m long lengths of CORC® wire (CORC®-W3) were manufactured by ACT and wound into the two-layer magnet CCT-C1 at LBNL for which the mandrels were prepared from 3D printed Accura® Bluestone® [69] (figure 56). The layers of the magnet were not impregnated. The two layers were assembled and the CORC® wires were connected in series. The magnet was tested at 4.2 K up to a current of 4.5 kA where the initial voltage rise indicated the start of the superconducting transition. At this current, a dipole field of about 1.1 T was measured (figure 57). The current was not increased further to reach I_c, or quench, as a safety precaution that would ensure further measurements of field quality before and after epoxy impregnation could be carried out. The

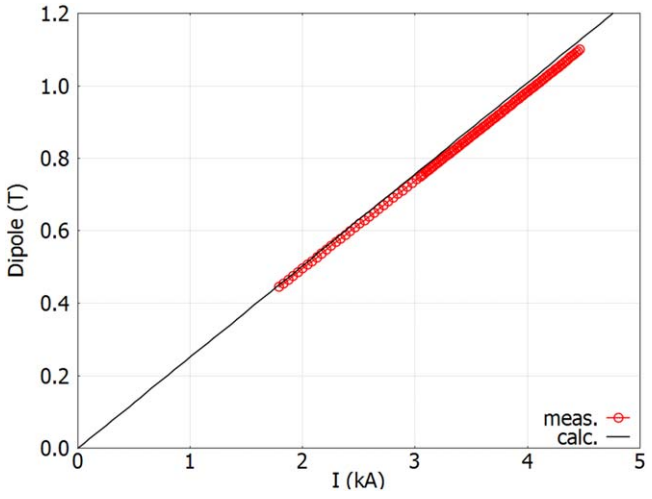

Figure 57. Dipole field of magnet CCT-C1 measured at 4.2 K as a function of current.

results of the CCT-C1 coil development and tests are presented in more detail elsewhere [70].

The second step towards achieving the near-term goal of 5 T in a CCT magnet wound from CORC® wires is to wind a four-layer, 40-turns per layer, CCT magnet (CCT-C2) using a higher tape count CORC® wire. One of the concerns with high-tape count CORC® wires is that they may be less flexible than those containing fewer tapes. The dipole transfer function of a CCT magnet depends on the tilt angle at which

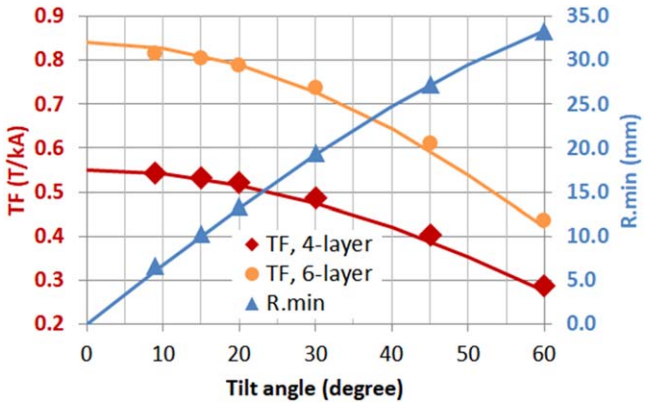

Figure 58. Dipole transfer function and minimum CORC® wire bending radius as a function of tilt angle for four-layer and six-layer CCT magnets with 70 mm aperture.

the wire is wound, which defines the minimum-bending radius of the wire at the poles, is shown for an aperture of 50 mm in figure 58. For the four-layer CCT-C2 magnet design, a tilt angle of 30° at an aperture of 70 mm was selected, which would result in a minimum-bending radius at the poles of 30 mm.

A two-layer, three-turn per layer sub-scale CCT magnet was prepared using wire CORC®-W5 containing 29 tapes to evaluate its performance at the bending radius at the poles of 30 mm. Figure 59 shows the CORC® wire I_c at 77 K before and after the wire was wound onto the mandrels, where I_c decreased from 1650 A to about 1240 A. The decrease is again caused mainly by the increased self-field on the wires after the layers were assembled. The sub-scale CCT magnet was also tested at 4.2 K, where it carried a current of about 12.4 kA (figure 59(b)). A total of 80 m of CORC® wire has recently been delivered to LBNL for winding into the four-layer magnet CCT-C2, which is expected to be wound and tested at LBNL before the end of 2018.

The final step to reach the short-term goal of 5 T is to develop a six-layer CCT magnet from high-J_e CORC® wires. The CORC® wires will most likely consist of tapes with 25 μm thick substrates that will become available at the end of 2018. The thinner substrates will allow smaller formers to be used in the CORC® wire, making them even more flexible while allowing higher currents and current densities (section 3.2.4). The thinner and more flexible CORC® wire would allow a higher transfer function in the order of 0.74 T kA^{-1} at a minimum bending radius of 20 mm (figure 58). The optimum CORC® wire design, followed by winding and testing magnet CCT-C3, is scheduled for 2019.

7. CORC® magnet feeder cables and wires

CORC® cables and wires are highly suitable for application as flexible high-current magnet feeders. HTS feeder cables are required for injecting current into high-field magnet inserts for which the stray magnetic field at the magnet terminals exceeds the operating range of typical LTS feeder cables such as NbTi, or where the feeders extend towards the current leads at elevated temperatures.

A pair of CORC® wires was prepared for the 32 T magnet that was successfully tested at the NHMFL [10], in which the CORC® feeder wires connect the lower end of the vapor-cooled leads to the bus-bars near the terminals of the REBCO insert coils. The peak magnetic field at the CORC® feeder termination closest to the insert magnet was about 23 T. Although the operating current was only 174 A, the CORC® feeder wires needed to withstand significant vertical movement of about 10 mm of the insert coil with respect to the top magnet flange during cool down and field ramping [71]. Bending of the feeders that would allow such movement was accommodated by including a bend into the feeder wires, while providing mechanical support against Lorenz forces using a G10 support structure of which part is shown in figure 60.

One of the concerns with bending the CORC® feeder wires while at cryogenic temperatures was that the wires may not be as flexible compared to room temperature and that the performance of the feeder wires would degrade with each longitudinal movement of the magnet. The CORC® feeder wire I_c was therefore measured each time after the terminals moved together by 20 mm, which is twice the distance required for the 32 T magnet, followed by moving them back into their original position while in liquid nitrogen (figure 61). After initial I_c degradation of about 3% after eight cycles, I_c remained unchanged up to the maximum number of 30 cycles (figure 62). The results confirmed that CORC® wires retain most of their performance even when bent while at cryogenic temperatures.

The CORC® feeder wires that were incorporated into the 32 T magnet at the NHMFL, in which they still perform successfully, only operate at a current of 174 A. Much higher operating currents are possible in CORC® magnet feeder cables or wires in which part of the feeder experiences a relatively high magnetic field, or where the feeders experience a significant temperature gradient along their length. Large temperature gradients may be present when the CORC® feeders connect to a high-field insert magnet operating at low temperature, such as 4.2 K, while they connect to the current leads at a temperature of 50–80 K.

8. Summary

Less than a decade since the introduction of the CORC® cable concept, and less than three years after the introduction of CORC® wires, have the CORC® conductors matured into practical conductors for high-field magnet and compact power cable applications. Major advances in low-resistance terminations that allow current to be injected homogeneously into each tape of the conductor allowed a rapid development of high-current CORC® cables and wires. The CORC® conductor development has resulted in high-quality, reliable conductors that can be bent to small diameters and that can withstand high mechanical stresses without significant performance degradation. They are now routinely manufactured

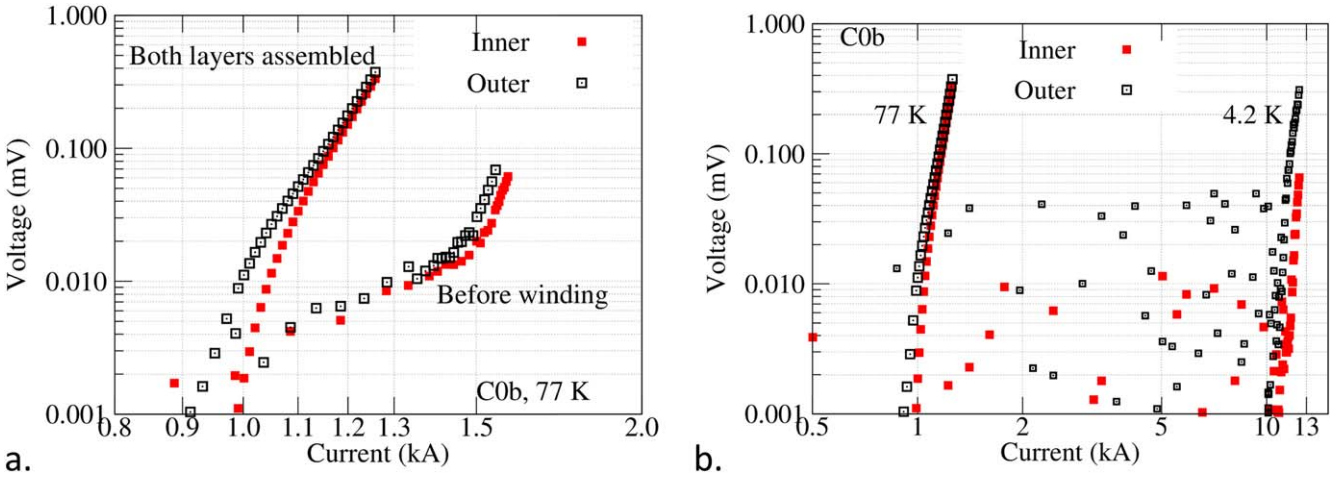

Figure 59. (a) Voltage as a function of current measured at 77 K in self-field before winding of wire CORC®-W5 and after being assembled into a two-layer, three-turn per layer CCT dipole magnet. (b) Voltage as a function of current at 77 and 4.2 K in self-field. Reproduced from [16]. © IOP Publishing Ltd. All rights reserved.

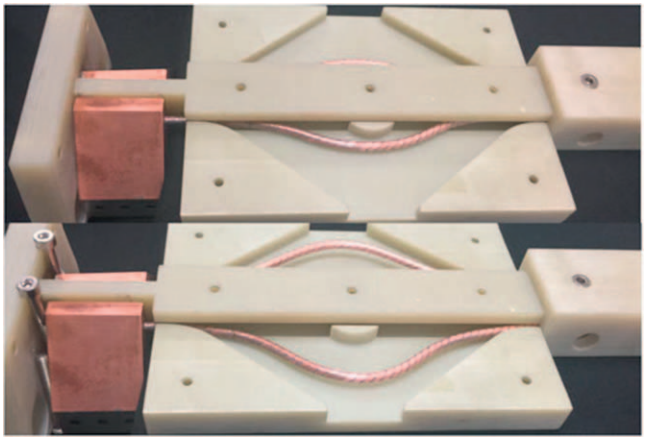

Figure 60. CORC® feeder wire in extended position (top), and in compressed position (bottom). © 2017 IEEE. Reprinted, with permission, from [71].

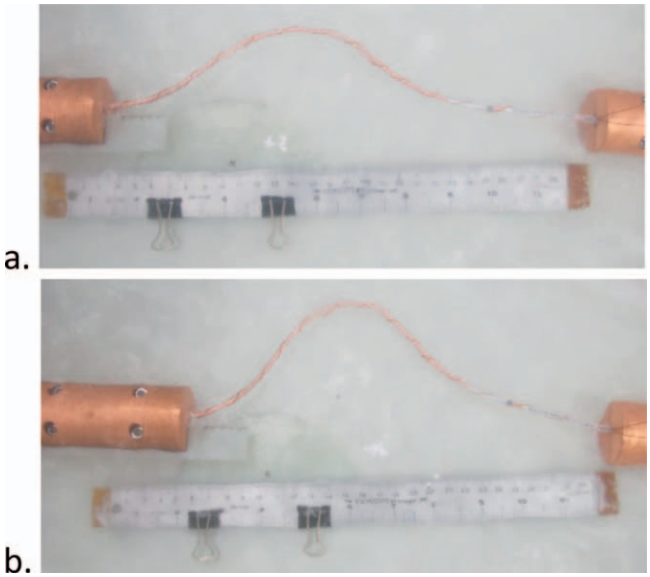

Figure 61. Testing of the CORC® feeder wire performance during bending in liquid nitrogen. (a) Extended CORC® feeder wire, and (b) feeder wire compressed by 20 mm.

in long lengths by Advanced Conductor Technologies and are in the process of demonstrating their capabilities in a wide range of applications.

Initial measurements of the performance limits of CORC® cables and wires under transverse compressive load, including cycling up to 100 000 cycles applied in liquid nitrogen, and under axial tensile stress, have been performed. The CORC® conductors proved to be highly resilient to mechanical stress, while several conductor optimization steps that would further increase the mechanical stress limits have been identified.

CORC® cables and wires are being developed for high-field magnets applications that require operating currents of 10–20 kA in a background field of 20 T, such as in particle accelerator magnets, while at the same time allowing engineering current densities exceeding 300 A mm^{-2}. These requirements have been met in CORC® wires where a J_e of over 400 A mm^{-2}, when extrapolated to 20 T, was demonstrated at a bending radius of 30 mm. Further improvement with respect to engineering current density at even smaller bending radii are expected in the near future with the introduction of even thinner CORC® wires containing tapes with 20–25 μm thick substrates. CORC® wires are now being incorporated into high-field accelerator magnets, such as in canted cosine-theta magnets. The program aims to demonstrate a 5 T CCT magnet by the end of 2019, followed by a demonstration of a 15–20 T CCT magnet in which a CORC® wire insert is operated within a LTS outsert magnet.

Fusion and particle detector magnets require even higher currents than accelerator magnets of between 50 and 100 kA in fields of 10–20 T, which can only be achieved when CORC® cables or wires are bundled into CICCs. CORC® cables have been configured into 6-around-1 CICCs and initial tests in the SULTAN test facility at the Paul Scherrer Institute have been performed. Further optimization of the 6-around-1 CORC®-CICC is underway, with the goal to

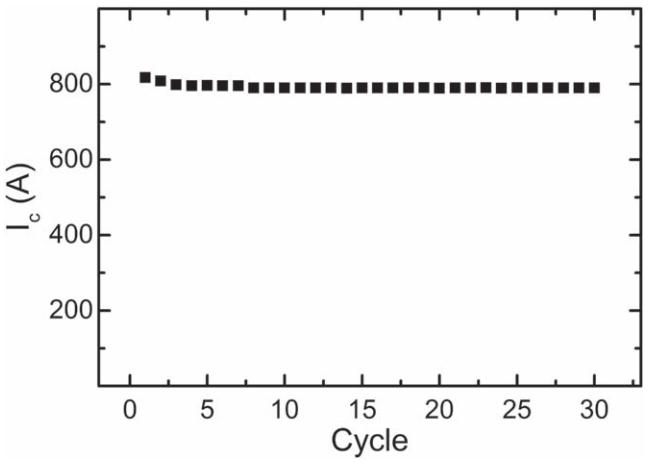

Figure 62. Critical current at 76 K of the CORC® feeder wire as a function of cycle between 10 and 30 mm longitudinal translation.

demonstrate degradation-free operation at 80 kA in a background field of 10.9 T.

The development of highly transposed CORC®-CICC for use in compact fusion magnets has recently began. The designs would allow for CICC bending to diameters of 1 m, while mechanical decoupling of the CORC® strands in the CICC would reduce the operating stresses on the strands.

CORC® cables have also been demonstrated successfully as dc power cables operating at 4 kA in pressurized helium gas and as FCL conductors that are able to quickly limit overcurrents and protect sensitive equipment. The CORC® cable and wire architecture allows for highly compact dc power systems that may include relatively tight bends, making them highly suitable for operation on board Navy ships, electric aircraft and in data centers.

Major developments on the conductor level of CORC® cables and wires, although ongoing, have resulted in a practical and reliable conductor for many applications. The next chapter of CORC® conductor development is about to be written, where development moves from a conductor level to a system level in which CORC® cables and wires are applied in high-field magnets for accelerators and fusion, and compact power cable systems for use in confined spaces.

Acknowledgments

This work has been supported in part by the US Navy under contracts N00024-14-C-4065 and N00014-15-P-1171 and by the US Department of Energy under contracts DE-SC0007660, DE-SC0009545, DE-SC0013723, DE-SC0014009, DE-SC0015775, DE-SC0018125 and DE-SC0018127. The authors like to thank Dima Abraimov and Ashleigh Francis from the Applied Superconductivity Center at the National High Magnetic Field Laboratory for performing the in-field measurements of REBCO tapes at 4.2 K, Tim Mulder and Herman ten Kate from CERN and the University of Twente for their effort in developing and testing of CORC®-CICCs for fusion and detector magnets, the researchers at the Paul Scherrer Institute for performing the CORC®-CICC tests in SULTAN, Xiaorong Wang and Hugh Higley from Lawrence Berkeley National Laboratory for their collaboration in developing CCT magnets using CORC® wires, and Chul Kim and Sastry Pamidi from the Center for Advanced Power Systems at the Florida State University and Lukas Graber from the Georgia Institute of Technology for their collaboration in developing helium gas cooled CORC® power cables.

ORCID iDs

D C van der Laan https://orcid.org/0000-0001-5889-3751
J D Weiss https://orcid.org/0000-0003-0026-3049

References

[1] Demko J A, Sauers I, James D R, Gouge M J, Lindsay D, Roden M, Tolbert J, Willén D, Træholt C and Nielsen C T , 2007 Triaxial HTS cable for the AEP Bixby project *IEEE Trans. Appl. Supercond.* **17** 2047–50
[2] Weber C S, Lee R, Ringo S, Masuda T, Yumura H and Moscovic J 2007 Testing and demonstration results of the 350 m long HTS cable system installed in Albany, NY *IEEE Trans. Appl. Supercond.* **17** 2038–42
[3] Maguire J, Folts D, Yuan J, Lindsay D, Knoll D, Bratt S, Wolff Z and Kurtz S 2009 Development and demonstration of a fault current limiting HTS cable to be installed in the Con Edison grid *IEEE Trans. Appl. Supercond.* **19** 1740–3
[4] Yanagisawa Y *et al* 2015 Combination of high hoop stress tolerance and a small screening current-induced field for an advanced Bi-2223 conductor coil at 4.2 K in an external field *Supercond. Sci. Technol.* **28** 125005
[5] Marshall W S, Bird M D, Godeke A, Larbalestier D C, Markiewicz W D and White J M 2017 Bi-2223 test coils for high-resolution NMR magnets *IEEE Trans. Appl. Supercond.* **27** 4300905
[6] Larbalestier D C *et al* 2014 Isotropic round-wire multifilament cuprate superconductor for generation of magnetic fields above 30 T *Nat. Mater.* **13** 375–81
[7] Fajardo L G, Brouwer L, Caspi S, Gourlay S, Prestemon S and Shen T 2018 Designs and prospects of Bi-2212 canted-cosine-theta magnets to increase the magnetic field of accelerator dipoles beyond 15 T *IEEE Trans. Appl. Supercond.* **28** 40008305
[8] Hazelton D W, Selvamanickam V, Duval J M, Larbalestier D C, Markiewicz W D, Weijers H W and Holtz R L 2009 Recent developments in 2G HTS coil technology *IEEE Trans. Appl. Supercond.* **19** 2218–22
[9] Yoon S, Kim J, Cheon K, Lee H, Hahn S and Moon S-H 2016 26 T 35 mm all-$GdBa_2Cu_3O_{7-x}$ multi-width no-insulation superconducting magnet *Supercond. Sci. Technol.* **29** 04LT04
[10] Weijers H W 2018 A marriage of high and low temperature superconductors: the 32 T magnet' *MST Seminar NHMFL (Tallahassee, FL, 24 January)*
[11] Majkic G, Mensah R J, Selvamanickam V, Xie Y-Y and Salama K 2009 Electromechanical behavior of IBAD/MOCVD YBCO coated conductors subjected to torsion and tension loading *IEEE Trans. Appl. Supercond.* **19** 3003–8
[12] Zhang Y, Hazelton D W, Kelley R, Kasahara M, Nakasaki R, Sakamoto H and Polyanskii A 2016 Stress–strain relationship, critical strain (stress) and irreversible strain (stress) of IBAD-MOCVD-based 2G HTS wires under uniaxial tension *IEEE Trans. Appl. Supercond.* **26** 8400406

[13] van der Laan D C 2009 $YBa_2Cu_3O_{7-\delta}$ coated conductor cabling for low AC-loss and high-field magnet applications *Supercond. Sci. Technol.* **22** 065013

[14] Weiss J D, Mulder T, ten Kate H J J and van der Laan D C 2017 Introduction of CORC® wires: highly flexible, round high-temperature superconducting wires for magnet and power transmission applications *Supercond. Sci. Technol.* **30** 014002

[15] van der Laan D C, Lu X F and Goodrich L F 2011 Compact $GdBa_2Cu_3O_{7-\delta}$ coated superconductor cables for electric power transmission and magnet applications *Supercond. Sci. Technol.* **24** 042001

[16] Wang X, Caspi S, Dietderich D R, Ghiorso W B, Gourlay S A, Higley H C, Lin A, Prestemon S O, van der Laan D and Weiss J D 2018 A viable dipole magnet concept with REBCO CORC® wires and further development needs for high-field magnet applications *Supercond. Sci. Technol.* **31** 045007

[17] van der Laan D C, Weiss J D, Kim C H, Graber L and Pamidi S 2018 Development of CORC® cables for helium gas cooled power transmission and fault current limiting applications *Supercond. Sci. Technol.* **31** 085011

[18] Zhou C, Yagotintsev K A, Gao P, Haugan T J, van der Laan D C and Nijhuis A 2016 Critical current of various REBCO tapes under uniaxial strain *IEEE Trans. Appl. Supercond.* **26** 8401304

[19] Cheggour N, Ekin J W, Clickner C C, Verebelyi D T, Thieme C L H, Feenstra R and Goyal A 2003 Reversible axial-strain effect and extended strain limits in Y–Ba–Cu–O coatings on deformation-textured substrates *Appl. Phys. Lett.* **83** 4223–5

[20] van der Laan D C, Abraimov D, Polyanskii A A, Larbalestier D C, Douglas J F, Semerad R and Bauer M 2011 Anisotropic in-plane reversible strain effect in $Y_{0.5}Gd_{0.5}Ba_2Cu_3O_{7-\delta}$ coated conductors *Supercond. Sci. Technol.* **24** 115010

[21] van der Laan D C and Ekin J W 2007 Large intrinsic effect of axial strain on the critical current of high temperature superconductors for electric power applications *Appl. Phys. Lett.* **90** 052506

[22] ten Haken B, Beuink A and ten Kate H H J 1997 Small and repetitive axial strain reducing the critical current in BSCCO/Ag superconductors *IEEE Trans. Appl. Supercond.* **7** 2034–7

[23] van der Laan D C, Douglas J F, Clickner C C, Stauffer T C, Goodrich L F and van Eck H J N 2011 Evidence that the reversible strain effect on critical current density and flux pinning in $Bi_2Sr_2Ca_2Cu_3O_x$ tapes is caused entirely by the pressure dependence of the critical temperature *Supercond. Sci. Technol.* **24** 032001

[24] Sugano M, Nakamura T, Manabe T, Shikimachi K, Hirano N and Nagaya S 2008 The intrinsic strain effect on critical current under a magnetic field parallel to the c axis for a MOCVD-YBCO-coated conductor *Supercond. Sci. Technol.* **21** 115019

[25] van der Laan D C, Ekin J W, Douglas J F, Clickner C C, Stauffer T C and Goodrich L F 2010 Effect of strain, magnetic field and field angle on the critical current density of $YBa_2Cu_3O_{7-\delta}$ coated conductors *Supercond. Sci. Technol.* **23** 072001

[26] van der Laan D C, Weiss J D, Noyes P, Trociewitz U P, Godeke A, Abraimov D and Larbalestier D C 2016 Record current density of 344 A mm^{-2} at 4.2 K and 17 T in CORC® accelerator magnet cables *Supercond. Sci. Technol.* **29** 055009

[27] Hazelton D 2018 Private communications

[28] Advanced Conductor Technologies LLC www.advancedconductor.com

[29] Sundaram A, Zhang Y, Knoll A R, Abraimov D, Brownsey P, Kasahara M, Carota G M, Nakasaki R, Camero J B and Schwab G 2016 2G HTS wires made on 30 μm thick Hastelloy substrate *Supercond. Sci. Technol.* **29** 104007

[30] Takayasu M, Chiesa L, Bromberg L and Minervini J V 2011 Cabling method for high current conductors made of HTS tapes *IEEE Trans. Appl. Supercond.* **21** 2340–4

[31] Makoto Takayasu F J, Mangiarotti L, Chiesa L, Bromberg and Minervini J V 2013 Conductor characterization of YBCO twisted stacked-tape cables *IEEE Trans. Appl. Supercond.* **23** 4800104

[32] Uglietti D, Wesche R and Bruzzone P 2014 Design and strand tests of a fusion cable composed of coated conductor tapes *IEEE Trans. Appl. Supercond.* **24** 4800704

[33] Uglietti D, Bykovsky N, Sedlak K, Stepanov B, Wesche R and Bruzzone P 2015 Test of 60 kA coated conductor cable prototypes for fusion magnets *Supercond. Sci. Technol.* **28** 124005

[34] Celentano G, De Marzi G, Fabbri F, Muzzi L, Tomassetti G, Anemona A, Chiarelli S, Seri M, Bragagni A and della Corte A 2014 Design of an industrially feasible twisted-stack HTS cable-in-conduit conductor for fusion application *IEEE Trans. Appl. Supercond.* **24** 4601805

[35] Augieri A *et al* 2015 Electrical characterization of ENEA high temperature superconducting cable *IEEE Trans. Appl. Supercond.* **25** 4800704

[36] Wolf M J, Fietz W H, Bayer C M, Schlachter S I, Heller R and Weiss K-P 2016 HTS CroCo: a stacked HTS conductor optimized for high currents and long-length production *IEEE Trans. Appl. Supercond.* **26** 6400106

[37] Wolf M J, Bagrets N, Fietz W H, Lange C and Weiss K-P 2018 Critical current densities of 482 A mm^{-2} in HTS crossconductors at 4.2 K and 12 T *IEEE Trans. Appl. Supercond.* **28** 4802404

[38] Yanagi N, Ito S, Terazaki Y, Seino Y, Hamaguchi S, Tamura H, Miyazawa J, Mito T, Hashizume H and Sagara A 2015 Design and development of high-temperature superconducting magnet system with joint-winding for the helical fusion reactor *Nucl. Fusion* **55** 053021

[39] Terazaki Y, Yanagi N, Ito S, Seino Y, Hamaguchi S, Tamura H, Mito T, Hashizume H and Sagara A 2015 Measurement and analysis of critical current of 100-kA class simply-stacked HTS conductors *IEEE Trans. Appl. Supercond.* **25** 4602905

[40] Takayasu M, Chiesa L, Allen N C and Minervini J V 2016 Present status and recent developments of the twisted stacked-tape cable conductor *IEEE Trans. Appl. Supercond.* **26** 6400210

[41] Li Z Y, Li Y Q, Wang M Y, Xi D M, Zhang J W, Ma Y H, Hong Z, Jin Z and Ryu K 2018 Evaluation of electrical and mechanical characteristics for a twisted soldered-stacked-square (3S) HTS wire with 1 mm width *IEEE Trans. Appl. Supercond.* **28** 4800405

[42] Goldacker W, Nast R, Kotzyba G, Schlachter S I, Frank A, Ringsdorf B, Schmidt C and Komarek P 2006 High current DyBCO-ROEBEL assembled coated conductor (RACC) *J. Phys.: Conf. Ser.* **43** 901

[43] Badcock R A, Long N J, Mulholland M, Hellmann S, Wright A and Hamilton K A 2009 Progress in the manufacture of long length YBCO Roebel cables *IEEE Trans. Appl. Supercond.* **19** 3244–7

[44] Goldacker W, Grilli F, Pardo E, Kario A, Schlachter S I and Vojenčiak M 2014 Roebel cables from REBCO coated conductors: a one-century-old concept for the superconductivity of the future *Supercond. Sci. Technol.* **27** 093001

[45] Kirby G A *et al* 2017 First cold powering test of REBCO Roebel wound coil for the EuCARD2 future magnet

development project *IEEE Trans. on Appl. Supercond.* **27** 1–7
[46] Kario A, Vojenciak M, Grilli F, Kling A, Ringsdorf B, Walschburger U, Schlachter S I and Goldacker W 2013 Investigation of a Rutherford cable using coated conductor Roebel cables as strands *Supercond. Sci. Technol.* **26** 085019
[47] Willering G P, van der Laan D C, Weijers H W, Noyes P D, Miller G E and Viouchkov Y 2015 Effect of variations in terminal contact resistances on the current distribution in high-temperature superconducting cables *Supercond. Sci. Technol.* **28** 035001
[48] van der Laan D 2017 Superconducting cable connections and methods *US Patent* 9755329
[49] Mulder T, Weiss J, van der Laan D , Dhalle M and Kate H ten 2018 Development of ReBCO-CORC wires with current densities of 400 to 600 A mm^{-2} at 10 T and 4.2 K *IEEE Trans. Appl. Supercond.* **28** 4800504
[50] van der Laan D C, Noyes P, Miller G, Weijers H and Willering G 2013 Characterization of a high-temperature superconducting conductor on round core cables in magnetic fields up to 20 T *Supercond. Sci. Technol.* **26** 045005
[51] van der Laan D C, Goodrich L F, Noyes P, Trociewitz U P, Godeke A, Abraimov D, Francis A and Larbalestier D C 2015 Engineering current density in excess of 200 A mm^{-2} at 20 T in CORC® magnet cables containing RE-$Ba_2Cu_3O_{7-\delta}$ tapes with 38 μm thick substrates *Supercond. Sci. Technol.* **28** 124001
[52] Fleiter J, Ballarino A, Bottura L and Tixador P 2013 Electrical characterization of REBCO Roebel cables *Supercond. Sci. Technol.* **26** 065014
[53] Fleiter J, Ballarino A, Bottura L, Goldacker W and Kario A 2015 Characterization of Roebel cables for potential use in high-field magnets *IEEE Trans. Appl. Supercond.* **25** 4802404
[54] van der Laan D C, McRae D M and Weiss J D 2019 Effect of transverse compressive monotonic and cyclic loading on the performance of superconducting CORC® cables and wires *Supercond. Sci. Technol.* **32** 015002
[55] Bayer C M, Gade P V, Barth C, Preuß A, Jung A and Weiß K P 2016 Mechanical reinforcement for RACC cables in high magnetic background fields *Supercond. Sci. Technol.* **29** 025007
[56] Otten S, Dhallé M, Gao P, Wessel W, Kario A, Kling A and Goldacker W 2015 Enhancement of the transverse stress tolerance of REBCO Roebel cables by epoxy impregnation *Supercond. Sci. Technol.* **28** 065014
[57] Bykovsky N, Uglietti D, Wesche R and Bruzzone P 2016 Design optimization of round strands made by twisted stacks of HTS tapes *IEEE Trans. Appl. Supercond.* **26** 4201207
[58] van der Laan D C, McRae D M and Weiss J D 2018 Effect of monotonic and cyclic axial tensile stress on the performance of superconducting CORC® wires *Supercond. Sci. Technol.* submitted
[59] Gouge M J *et al* 2009 Testing of 3-meter prototype fault current limiting cables *IEEE Trans. Appl. Supercond.* **19** 1744–7
[60] Tixador P and Nguyen N T 2012 Design of ReBaCuO-coated conductors for FCL *Supercond. Sci. Technol.* **25** 014009
[61] Weiss J D, Kim C, Pamidi S and van der Laan D C 2019 Hybrid superconducting fault current limiting CORC® wires with millisecond response time *Supercond. Sci. Technol.* **32** 034005
[62] Mulder T, Dudarev A, Mentink M, Silva H, van der Laan D, Dhallé M and ten Kate H 2016 Design and manufacturing of a 45 kA at 10 T REBCO-CORC cable-in-conduit conductor for large-scale magnets *IEEE Trans. Appl. Supercond.* **26** 4803605
[63] Mulder T, van der Laan D, Weiss J D, Dudarev A, Dhalle M and ten Kate H H J 2017 Design and preparation of two ReBCO-CORC® cable-in-conduit conductors for fusion and detector magnets *IOP Conf. Ser.: Mater. Sci. Eng.* **279** 012033
[64] Mulder T 2018 Advancing ReBCO-CORC wire and cable-in-conduit conductor technology for superconducting magnets *PhD Dissertation* University of Twente
[65] Commonwealth Fusion Systems www.cfs.energy
[66] Tri-Alpha Energy Technologies, Inc. https://tae.com
[67] Tokamak Energy www.tokamakenergy.co.uk
[68] Caspi S *et al* 2014 Canted-cosine-theta magnet (CCT)-a concept for high field accelerator magnets *IEEE Trans. Appl. Supercond.* **24** 4001804
[69] 3D Systems https://3dsystems.com/materials/accurabluestone)
[70] Wang X *et al* 2018 *Supercond. Sci. Technol.* submitted
[71] Voran A, Weijers H W, Markiewicz W D, Gundlach S R, Jarvis J B and Sheppard W R 2017 Mechanical support of the NHMFL 32 T superconducting magnet *IEEE Trans. Appl. Supercond.* **27** 4300305